Conserved traits of spiralian development in the bryozoan *Membranipora membranacea*

Bruno C. Vellutini[1], José M. Martín-Durán[1], Andreas Hejnol[1]

[1]Sars International Centre for Marine Molecular Biology, University of Bergen, Thormøhlensgate 55, 5006 Bergen, Norway.

Abstract

Background: Spiral cleavage is a remarkably conserved pattern of embryogenesis present in animals of the clade Spiralia, such as annelids, molluscs, flatworms and nemerteans. However, not all spiralians display spiral cleavage. Recent phylogenies suggest that the spiral arrangement of embryonic blastomeres is an ancestral trait for the Spiralia and that it was secondarily modified in several spiralian lineages, such as gastrotrichs, brachiopods and bryozoans. To better understand the evolution of cleavage patterns in relation to blastomere fate maps and embryonic gene expression, we describe the cell lineage and molecular patterning in the embryogenesis of the bryozoan *Membranipora membranacea*.

Results: *M. membranacea* develops through a unique stereotypic cleavage pattern with biradial symmetry and an embryo organized in identical quadrants with synchronous cell divisions. The quadrant identities are established as early as the 28-cell stage, when one vegetal blastomere (3D) activates the MAPK pathway, marking the future posterior region of the larva. Cells from this posterior quadrant divide asynchronously in subsequent stages leading to the morphological differentiation between quadrants. The first quartet of *M. membranacea* gives rise to the apical organ and ciliated band, the second and third quartet forms the oral/anal ectoderm, the fourth quartet the mesoderm and the vegetal blastomeres form the endoderm. We found that the early embryonic organization and the fate map of these early blastomeres in the bryozoan embryo are similar to a typical spiral-cleaving embryo. Furthermore we observe that correspondent blastomeres between the bryozoan and spiral-cleaving embryos share similar molecular identities, as revealed by the activity of MAPK and the expression of *otx* and *foxa*. The development of *M. membranacea* mainly differs from spiral-cleaving embryos in the downstream portions of the cell lineage, and in the origin of the mesoderm, which is formed by multiple fourth quartet blastomeres.

Conclusions: The similarity between the fate map of *M. membranacea* and spiral-cleaving embryos indicates that the cleavage geometry of the bryozoan evolved decoupled from other spiralian developmental traits. In this case, the blastomere fates remained evolutionarily conserved despite the drastic modification in the cleavage pattern from spiral to biradial. These findings suggest that blastomere fates of spiral-cleaving embryos might not be linked to the stereotypic spiral cleavage pattern, but depend on other factors, such as the underlying molecular patterning. Our comparative analysis on the bryozoan reveals yet another facet of how early development evolves and helps to shed some light into the developmental diversity of spiralians.

Keywords

Bryozoa, cyphonautes, spiral cleavage, cell lineage, larva, MAPK, molecular patterning.

Background

Molluscs, annelids, nemerteans and polyclad flatworms great diversity of adult forms, and yet share a remarkably similar embryogenesis (Child, 1897; Child, 1900; Conklin, 1897; Lillie, 1895; Surface, 1907; Treadwell, 1901; Wilson, 1892; Wilson, 1903; Zeleny, 1904). In these groups, the blastomeres at the 4-cell stage divide with the mitotic spindles oblique to the animal-vegetal axis, alternating direction (clockwise and counterclockwise) at each division cycle. Viewed from the animal pole, the symmetry of cleaving blastomeres was described as spiral, as opposed to the radial symmetry found in sea urchins, and this developmental pattern became known as *spiral cleavage* (Wilson, 1892). This pattern is stereotypic and the fate of individual blastomeres can be followed and compared across taxa. Such cell lineage studies revealed that animals with spiral cleavage not only share the spiral blastomere arrangement, but also have similar blastomere identities and a similar embryonic fate map (Hejnol, 2010).

Spiral cleavage is only found within the Spiralia, a major protostome clade sister to the Ecdysozoa (e.g. insects) (Dunn et al., 2014). Molluscs, annelids, nemerteans and polyclad flatworms are considered to have spiral cleavage and will be referred to as spiral-cleaving groups. Some spiralians (i.e. animals belonging to the clade Spiralia) such as gnathostomulids (Riedl, 1969), phoronids (Pennerstorfer and Scholtz, 2012) and entoprocts (Marcus, 1939; Merkel et al., 2012), also display a spiral symmetry but their blastomere identities and embryonic fate map have not been studied. Other clades – bryozoans, brachiopods, gastrotrichs and rotifers – do not show oblique cell divisions (Wanninger, 2015), while micrognathozoan embryos have never been observed (Figure 1). Mapping the spiral arrangement of embryonic blastomeres in the latest phylogenetic analysis (Laumer et al., 2015) indicates that spiral symmetry is likely ancestral to the clade composed of Lophotrochozoa and Rouphozoa (Figure 1). This implies the spiral cleavage pattern was modified during the evolution of gastrotrichs, brachiopods and bryozoans, as well as in other lineages within spiral-cleaving groups such as cephalopods (Wadeson and Crawford, 2003) and most platyhelminthes (Martín-Durán and Egger, 2012).

Bryozoans are sessile colonial invertebrates found in oceans worldwide. Phylactolaemata, Stenolaemata and Gymnolaemata – the main lineages of Bryozoa (Waeschenbach et al., 2012) – have fairly distinct developmental patterns regarding reproduction (e.g. brooding versus external development), early development (e.g. cleavage and gastrulation) and larval stages (Reed, 1991; Zimmer, 1997). None of the species investigated so far display a spiral arrangement of embryonic blastomeres (Reed, 1991). While phylacto- and stenolaemate develop via polyembryony and irregular cleavage – patterns of embryogenesis considered to be derived – the gymnolaemate bryozoans display a unique stereotypic cleavage pattern with biradially arranged blastomeres, a pattern widely conserved within the group.

Early embryological studies conducted by Barrois (1877), Prouho (1892), Calvet (1900), Pace (1906), Marcus (1938) and Corrêa (1948) found that the animal-most blastomeres of gymnolaemate embryos originate the apical disc and aboral epithelium

of the larva, the animal micromeres at the equator of the embryo form the ciliated band, and the vegetal cells produce the oral epithelium and endomesoderm (reviewed in Hyman, 1959; Reed, 1991; Zimmer, 1997). However, cleavage patterns have only been systematically followed until the 64-cell stage (Corrêa, 1948; Pace, 1906) and, as of today, there is no complete cell lineage of a bryozoan larva. Several basic questions remain unsolved. For example, the relation between the embryonic animal/vegetal axis and the larval body axes is unclear (Nielsen, 2005), and the fate of the blastopore remains to be confirmed (Gruhl, 2009; Marcus, 1938; Prouho, 1892; Zimmer, 1997). Finally, the fate of internalized cells has not been traced (Zimmer, 1997) and the source of mesoderm remains a specially contentious topic (Gruhl, 2009).

In this study, we address the open questions about bryozoan development by investigating the cosmopolitan gymnolaemate species *Membranipora membranacea* (Linnaeus, 1767). By tracing the cell lineage with 4D microscopy, we identify the embryonic origin of the tissues of a typical cyphonautes larva and compare our findings to the spiral cleavage developmental pattern. In addition, we combine the cell lineage data with the analysis of gene expression and MAPK activity to base our comparison not only on the end fate of a cell, but also on the molecular identity of the blastomeres during all developmental stages. Our work reveals similarities in the fate and molecular maps of the bryozoan and spiral-cleaving embryos that – based on the phylogenetic position of bryozoans – can be interpreted as conserved traits of spiralian development. Furthermore, it suggests that cleavage patterns can be modified without major changes in the identity of blastomeres and cell fates. Our study highlights the power of the comparative approach to address fundamental questions of development and evolution such as the relation between cleavage patterns and fate maps.

Results

General development

Colonies of *M. membranacea* spawn fertilized discoidal eggs into the water column (Temkin, 1994). Released eggs undergo activation, becoming spherical, and initiate cleavage with a discernible accumulation of yolk in the vegetal pole (Figure 2A–B). Vegetal yolky cells are internalized during gastrulation (Figure 2C–E; Figure 2J–M) and by mid-gastrula stage the primordium of the apical organ (apical disc) and of the ciliated band (corona) are visible (Figure 2E). The vegetal plate invaginates and the embryo elongates along the animal-vegetal axis forming a late gastrula with clearly defined larval structures (i.e. apical organ, shell, gut and corona) (Figure 2F–G). At this point the fertilization envelope opens at the apical and basal ends and the embryo begins to swim by ciliary beating (Figure 2F). The internal cavity (vestibule) widens in the anteroposterior axis resulting in the typical laterally compressed, triangular shaped and shelled feeding larva of gymnolaemate bryozoans – the cyphonautes (Figure 2H–I) (Stricker et al., 1988). In this study, we recorded and traced the cell lineage from the 2-cell stage (Figure 2B) until the late gastrula stage (Figure 2G).

Cleavage pattern and embryonic axes

The cleavage of *M. membranacea* is biradial as previously described for gymnolaemates (Figure 3) (Gruhl, 2009; Nielsen, 2005; Reed, 1987; Reed, 1991; Zimmer, 1997). The first cell division occurs between 1–2 hours post activation (hpa) and originates two equal blastomeres with a meridional cleavage furrow. The second division is also meridional and perpendicular to the first, resulting in four identical blastomeres

at 3 hpa with an unequal animal/vegetal distribution of yolk (Figure 2B; Figure 3; Figure 4, 4-cell). We labeled the blastomere that originates the posterior structures of the larval body as "D" (see Figure 5 for fate map overview and "Methods" for nomenclature details). At 4 hpa, an equatorial third division gives rise to four animal blastomeres with little yolk content (1a–1d) and four equally sized vegetal blastomeres with a greater amount of yolk in the central portion of the embryo (1A–1D) (Figure 2C; Figure 3; Figure 4, 8-cell). On the next division at 5.2 hpa, each animal blastomere divides parallel to the plane of the first cleavage resulting in four inner and four outer cells; vegetal blastomeres cleave in the same manner slightly after (Figure 3; Figure 4, 16-cell). At the 16-cell stage, yolk-rich cells (2A–2D) lie inner to the outer vegetal cells of the second quartet (2a–2d) and the embryo is clearly biradial.

On subsequent stages, the eight animal blastomeres of *M. membranacea* act as octets, synchronized in the cell divisions (Figure 3). The first octet (animal pole cells 1q, 4 inner and four outer cells) divide equatorially making a brief 24-cell stage and the octets $1q^1$ and $1q^2$ (6.5 hpa). This division is shortly followed by an unequal cleavage originating the third quartet (3a–3d) from the four inner vegetal blastomeres at 6.8 hpa (Figure 3; Figure 4, 28-cell). Outer vegetal cells of the second quartet (2q) divide parallel to the second division at 7.5 hpa, resulting in twelve outer vegetal cells (3a–3d, $2a^R$–$2d^R$, $2a^L$–$2d^L$) that surround four large blastomeres in the vegetal plate (3A–3D) at the 32-cell stage. At 8 hpa, the top animal octet ($1q^1$) divides forming a 40-cell embryo (Figure 3; Figure 4, 40-cell). Finally, the vegetal most animal octet ($1q^2$) divides meridionally at 8.6–9 hpa forming an equatorial row of cells above the vegetal blastomeres (Figure 3; Figure 4, 48-cell).

Cell divisions between the correspondent blastomeres of each quartet are mostly synchronous up to the 64-cell stage (Figure 4). At this point, we observe the fist two significant asynchronous cell divisions in the posterior D quadrant (Figure S1). The cell $1d_i^{12}$ divides approximately 1h before than its partners $1a_i^{12}$, $1b_i^{12}$ and $1c_i^{12}$ (Figure S1), while the cell $1d_e^{11}$ divides 2h later than its quartet correspondents $1a_e^{11}$, $1b_e^{11}$ and $1c_e^{11}$ (Figure 4 and Figure S1). Other cells from the D quadrant also exhibit asynchrony, such as the large inner vegetal blastomeres 3Q (3D is delayed) and the outer vegetal cells 3q (3c is delayed). At a similar time point we observe the first difference in the orientation of the cleavage plane between quartet cells, whereas $1d_e^{12}$ divides equatorially, $1a_e^{12}$, $1b_e^{12}$ and $1c_e^{12}$ divide meridionally. These events are the first morphological evidence for the break in the biradial symmetry of the bryozoan embryo.

Larval fates

The larval body of *M. membranacea* develops from the four quadrants in a symmetrical manner, each lineage contributing almost equally to the structures on their respective sides: D=posterior, C=right, B=anterior and A=left (Figure 5A).

Progeny of the first quartet of animal blastomeres (1a–1d) originates apical ectodermal structures such as the apical organ, the aboral epithelia and the corona (Figure 5A). The apical organ is derived from derivatives of the apical-most cells $1a^1$, $1c^1$ and $1d^1$ (Figure 5B; Figure 6A). Cells 1a and 1c form the lateral and anterior most portion of the apical organ while the posterior cell 1d contributes not only to the posterior portion, but also to the tissues at the base of the apical organ (Figure 6A). Thus, the cell 1b is the only blastomere of the first animal quartet that does not contribute to the apical organ. Epithelial cells between the apical organ and the corona are mostly derived from the octets $1q^{11}$ and $1q^{12}$. Outer coronal cells correspond to $1q^{12}$ and $1q^2$

while inner coronal cells (turned inwards after the invagination of the vegetal plate) are derived from $1q^2$ (Figure 6A). For a detailed overview of cell fates see Figure S2.

Vegetal blastomeres (1A–1D) form the epithelium of the vestibule, the oral/anal ectoderm as well as the cells internalized during gastrulation, which originate the endoderm and mesoderm of the cyphonautes larva (Figure 5A). The cellular arrangement at the vegetal plate in a 40-cell embryo consists of 12 outer cells (3a–3d, $2a^{R/L}$–$2d^{R/L}$) and four large inner blastomeres (3A–3D) (Figure 6B). Here we define gastrulation as the internalization of these four vegetal cells. It occurs by delamination and epiboly in two rounds of division of the outer vegetal twelve-tets, which divide radially, pushing the 4 larger blastomeres internally and outlining a blastopore (Figure 6B, 90 cell). At the 90-cell stage 12 cells are defining the blastopore lip, but this number gets reduced to 8 cells after the next division (Figure 6B, 120 cell). From the 12 vegetal cells, one does not divide ($3c^2$) and continue to line the right side of the blastopore lip (Figure 6B, 120 cells). Cells at the vertices of the blastopore on the 90-cell stage ($2a^{L2}$, $2b^{R2}$, $2c^{L2}$ and $2d^{R2}$) get pushed away from the blastopore lip, which now consists of 8 cells (Figure 6B). Blastomeres not forming the blastoporal lip also undergo the same round of two radial divisions except for $3c^1$, the sister of $3c^2$. The derivatives of these 12 vegetal outer blastomeres form the whole ectoderm that invaginates and develops into the epithelia of the vestibule and preoral funnel. Thus, during the invagination of the vegetal plate and the apical basal elongation of the embryo, the fate of the blastopore in *M. membranacea* is the larval mouth.

During epiboly (90 cell), three of the internalized large blastomeres (3A–3C) undergo a round of unequal division forming the basal cells 4a–4c and the apical cells 1A–1C (Figure 6C). The division of the cell 3D occurs 3h delayed in comparison to the other blastomeres. This round of division sets apart the endoderm (4A–4D) from the mesodermal tissues (4a–4d) of *M. membranacea* cyphonautes larva. The cells 4a and 4c divide twice anteroposteriorly forming a pair of lateral rows of mesodermal cells (Figure 6C). The most anterior cells ($4a^A$ and $4c^A$) form a bilateral pair of muscle cells extending from the corona to the apical organ (Figure 7). Interestingly, one anterolateral cell ($4a^{A1}$) migrates from the corona level until the apical organ during apical/basal elongation of the embryo. At the frontal portion of the larva, the cell 4b divides forming a column of cells stacking from the corona until the apical organ; the identity or role of these cells is unknown (Figure 6C). We could not resolve the fate of the 4d cell. Blastomeres 4A and 4C undergo anteroposterior divisions while 4B divides meridionally lining up with the blastoporal opening and forming the endodermal tissues of the cyphonautes larva (Figure 6C; Figure 7).

MAPK activity

The asymmetric activation of the MAPK pathway in spiralian embryos suggests that this molecular signaling might be involved in the establishment of the dorsal organizer (Lambert and Nagy, 2001). So far, all investigated molluscs show activated MAPK in the 3D blastomere (Henry and Perry, 2007; Koop et al., 2007; Lambert and Nagy, 2001; Lambert and Nagy, 2003). *M. membranacea* does not show MAPK activity in any of the blastomeres up to the 16-cell stage (Figure 8A). We first detect activated MAPK in the 3D vegetal blastomere at the 28-cell stage (Figure 8B). MAPK activity persists at the 3D cell from the 28–90-cell stage and fades prior to the 3D division around 90-cell stage (Figure 8B–D). MAPK activity is not continued in the progeny of 3D, 4D or 4d (Figure 8E–F) and was not detected in later embryonic stages.

Gene expression

In order to complement the cell lineage studies and to better understand the body patterning of cyphonautes larvae, we analyzed the expression of sixteen conserved molecular markers during the development of *M. membranacea* (Figure 9–12): anterior/neural (*six3/6*, *dlx*, *otx2*, *pax6* and *nk2.1*), foregut (*foxa* and *gsc*), germline (*nanos*), hindgut/posterior (*bra*, *cdx*, *evx* and *wnt1*), endodermal (*gata456*) and mesodermal (*twist*, *foxc* and *foxf*) markers.

We first detected transcripts of *six3/6* in *M. membranacea*, a transcription factor associated to anterior neural patterning (Marlow et al., 2014; Steinmetz et al., 2010), during early gastrulation in one outer lateral vegetal plate cell ($2c^{R2}$), one anterior endomesodermal cell (4B) and in 5 cells of the apical disc (Figure 9; Figure 11A). Expression of *six3/6* clears from $2c^{R2}$ and 4B, but persists in the inner cells of the forming apical organ, a central neural region occupied by serotonergic-positive cells in other cyphonautes larvae (Nielsen and Worsaae, 2010). We detected *dlx* transcripts, a gene involved in neurogenesis and proximodistal patterning (Panganiban and Rubenstein, 2002), in the 8 animal pole cells of the 16 cell stage (1q), broadly in the apical disc during gastrulation and elongation and, finally, localized to the whole apical organ in the late gastrula (Figure 9). The gene *otx2* is also involved in anterior neural patterning (Marlow et al., 2014; Steinmetz et al., 2010). It is expressed in all blastomeres between 2–8-cell stage and gets restricted to the apical octet of the 16-cell stage (Figure 9). At the 32-cell stage, *otx2* transcripts localize to the $1q^2$ octet and during gastrulation there are 3 rows of cells expressing *otx* with a posterior gap (Figure 11B). During mid-gastrula two cells in the apical organ express transcripts of *otx2* (Figure 11B). In the late larva, *otx2* is expressed in the corona and vestibule epithelium (Figure 11B). Expression of *pax6* is first detected during gastrulation, in bilateral patches of the apical ectoderm, and remains as a thin line of expression encircling the embryo above the corona (Figure 9). The gene *nk2.1* is involved in the patterning of the neural plate in vertebrates (Shimamura et al., 1995) and is expressed in anterior and ventral territories including the apical/neural plate and anterior endoderm (Lowe et al., 2003; Marlow et al., 2014; Takacs et al., 2004; Venkatesh et al., 1999). Transcripts of *nk2.1* are present in the progeny of the vegetal cells 2b and 3b in the early gastrula stage (Figure 9). These cells occupy an anterior vegetal position abutting the anterior blastopore lip until the edge of the vegetal plate. After the invagination of the vegetal plate, *nk2.1*-positive cells are lining the anterior portion of the preoral funnel, next to the mouth.

Expression of *foxa* is related to endoderm specification and commonly associated with the blastopore lip and foregut (Arenas-Mena, 2006; Boyle and Seaver, 2010; Oliveri et al., 2006). At the 16-cell stage, we detected faint expression of *foxa* in the outer vegetal blastomeres and in 10 (out of 12) cells surrounding the 4 large blastomeres at the 32-cell stage (2q and 3q, except posterior cells $2d^L$ and $2d^R$) (Figure 9; Figure 11C). Expression of *foxa* persisted in the daughter cells of the next division forming 2 rows of cells around the blastopore with a gap at the posterior end (Figure 11C). With the invagination of the vegetal plate, this region occupies an anterior/lateral position in the vestibule wall, surrounding the mouth region of the late gastrula (Figure 9; Figure 11D). We only found transcripts of *gsc* at the early gastrula stage in two anterior and a bilateral pair of cells at the vegetal plate (Figure 9; Figure 11E). In the late gastrula, *gsc* is expressed in bilateral domains of the vestibule wall which fuse anteriorly.

The germline marker *nanos* (Extavour and Akam, 2003; Juliano et al., 2010) is expressed in two posterior cells of the vegetal plate at the 32-cell stage ($2d^{L}$ and 3d) (Figure 9). In subsequent stages, *nanos* continues restricted to two cells at the posterior portion of the vegetal plate, localizing to the internal sac region of the cyphonautes larva (Figure 11F).

All posterior/hindgut and mesodermal markers only initiate expression during gastrulation. The gene *bra* is related to blastopore, mesoderm and posterior/hindgut patterning (Technau, 2001). Expression of *M. membranacea bra* in the early gastrula occurs at the vegetal plate in a posterior band of cells near the blastopore lip (Figure 10; Figure 11G). It localizes to 6–8 cells at the posterior end of the mid gastrula and a broad portion of the posterior and lateral vestibule ectoderm (Figure 11G). *M. membranacea bra* expression domain reaches the posterior portion of the preoral funnel as well as the future hindgut area of the larva (Figure 10). A single posterior vegetal plate cell ($2d^{R2}$) and its daughter cells ($2d^{R21}$ and $2d^{R22}$) express the posterior/hindgut markers *cdx* and *evx* at the early gastrula (Figure 10; Figure 11H; Figure 11J). During gastrulation, *cdx* and *evx* continue to be expressed at the posterior edge of the vegetal plate (Figure 10; Figure 11J; Figure 11L) and localize to the posterior vestibule ectoderm (hindgut) of the late gastrula (Figure 10; Figure 11L). At this stage, *evx* is also found in the posterior region of the gut (Figure 11L; Figure 11M). We also detected a transient *evx* expression in the two internalized blastomeres 4a and 4c of the early gastrula. Finally, *wnt1* is expressed in a row of 3–5 cells (including $2d^{L2}$, $2d^{R2}$ and $3d^{2}$) posterior to the blastopore during gastrulation (Figure 10; Figure 11N). At the late gastrula, *wnt1* is detected at the posterior-most vestibule ectoderm, positioned between the corona and hindgut (Figure 10; Figure 11N).

Expression of *twist*, a central regulator in mesoderm differentiation (Technau and Scholz, 2003), only occurs in a portion of embryos during the development of *M. membranacea*. We detected colorimetric signal in bilateral internalized cells of the early gastrula – possibly 4a, 4c or derivatives – as well as at the anterior end of the late gastrula (Figure 10; Figure 11O). Transcripts of *foxc*, commonly expressed in anterior and posterior mesodermal domains (Häcker et al., 1995; Passamaneck et al., 2015; Shimeld et al., 2010), are present in one unidentified posterior vegetal plate cell of the early gastrula and two similarly positioned cells during mid gastrulation (Figure 10). In the late gastrula, *foxc* expression is located in the internal sac area. The gene *foxf* is a transcription factor involved in mesoderm patterning and expressed mainly in visceral and anterior territories (Mazet et al., 2006; Passamaneck et al., 2015; Pérez Sánchez et al., 2002; Shimeld et al., 2010; Zaffran et al., 2001). In *M. membranacea* it is expressed in the mesodermal cell 4b in the early and mid gastrula stages (Figure 10). This cell divides in a ladder-like manner, from basal to apical, forming a distinct frontal row of mesodermal cells expressing *foxf* at the anterior portion of the late gastrula.

The vegetal 3D blastomere expresses the endomesodermal marker *gata456* (Patient and McGhee, 2002) at the 32-cell stage (Figure 10; Figure 11P). Expression expands to adjacent lateral blastomeres 4A and 4C in the early gastrula and continues to be expressed in the endodermal tissues forming the gut of the cyphonautes larva (Figure 10; Figure 11P).

Discussion

Onset of quadrant identities and MAPK activity

The blastomeres of *M. membranacea* at the 4-cell stage are of equal size and give rise to symmetric quadrants of the cyphonautes larval body. The future position of each quadrant cannot be distinguished by morphology before gastrulation because the embryo is biradial until 80 cells. However, we found earlier molecular asymmetries that already mark the axis of bilateral symmetry of the larva. The earliest markers are the MAPK pathway activation and the expression of *gata456* in one vegetal blastomere located in the quadrant that will give rise to the posterior region of the larva. These data indicate that the future position of each quadrant in *M. membranacea* is established as early as the 28-cell stage.

In spiral-cleaving embryos that have equal-sized blastomeres at the 4-cell stage, the future position of each quadrant is specified at a similar stage. In molluscs, for example, the interaction of the 3D macromere with the animal blastomeres at the 32-cell stage establishes the quadrant identities and the dorsoventral axis of the embryo (Biggelaar, 1977; Clement, 1962; Freeman and Lundelius, 1992; Gonzales et al., 2006; Martindale, 1986; Martindale et al., 1985). The MAPK pathway is the implicated molecular signaling underlying these events (Henry and Perry, 2007; Koop et al., 2007; Lambert and Nagy, 2001; Lambert and Nagy, 2003). The pattern of MAPK activation found in equal-cleaving molluscs (Table 1) (Koop et al., 2007; Lambert and Nagy, 2003) – a single posterior blastomere (3D) – is the same we observe in the bryozoan *M. membranacea*. The comparison suggests that equal-cleaving molluscs and bryozoans might share common patterning mechanisms during early development. Follow-up experiments testing the interaction between animal and vegetal blastomeres and the role of the MAPK pathway in the development of *M. membranacea* will help to elucidate the mechanisms for the specification of the quadrant identities in this bryozoan.

The activity and role of the MAPK pathway, however, is variable among spiral-cleaving groups. In annelids, MAPK is not active in the 3D macromere, but in the 4d cell of the equal-cleaving polychaete *Hydroides hexagonus* (Lambert and Nagy, 2003) and in the micromeres surrounding the blastopore of the unequal-cleaving annelids *Capitella teleta* and *Platynereis dumerilii* (Amiel et al., 2013; Pfeifer et al., 2014), and is not involved in the dorsoventral specification (Amiel et al., 2013; Pfeifer et al., 2014). Based on these observations, we suggest that the conspicuous 3D macromere MAPK activity and role in quadrant specification is not universal among spiralians or necessarily linked to the spiral cleavage pattern. Nevertheless, several spiralian groups, such as phoronids, nemerteans, polyclads, rotifers and gastrotrichs, lack any data on the MAPK pathway and should be investigated to better resolve the ancestral pattern and role of the MAPK signaling in spiralian development.

After the establishment of the quadrant identities, both the bryozoan *M. membranacea* and spiral-cleaving embryos show asynchronous cell divisions in the posterior quadrant. Such asynchrony also occurs in the D quadrant of the molluscs *Patella vulgata*, with the late division of the 3D cell (Biggelaar, 1977), and *Ilyanassa obsoleta* in the 1d derivatives (Clement, 1952; Goulding, 2009). In fact, spiral-cleaving embryos typically show asynchronous divisions in the D quadrant (Guralnick and Lindberg, 2001). This suggests that the specification of quadrant identities leads to differences in the cell cycle timing in both *M. membranacea* and spiral-cleaving embryos. Overall, the bryozoan embryo and equal-cleaving molluscs share a similar

pattern of MAPK activity, timing of quadrant specification and dynamics of cell divisions.

Blastomere homology and comparative fate maps

One fascinating aspect of spiral cleavage is that the pattern of cell divisions is conserved in such manner that it is possible to claim the homology of single embryonic blastomeres between distant animal clades (Conklin, 1897; Mead, 1897; Treadwell, 1901; Wilson, 1892; Wilson, 1898). Blastomeres can be compared by their position in the embryo, cell lineage (origin of blastomeres) and by their fates in the larval or adult tissues. Cell lineage studies revealed that putative homologous blastomeres share mostly-similar fates in various clades (Hejnol, 2010; Henry and Martindale, 1999; Lambert, 2010; Nielsen, 2004; Nielsen, 2005). Thus, cell lineage similarity has often been used to infer the homology of larval organs within spiral-cleaving embryos (Henry et al., 2007; e.g. Nielsen, 2005). Hereby we compare the cell lineage of the bryozoan *M. membranacea* to spiral-cleaving groups and discuss the evolutionary implications for the establishment of cell and organ homologies.

Apical organ

The apical organ of spiral-cleaving species is usually formed by the progeny of the apical-most $1q^1$ micromeres (Nielsen, 2004; Nielsen, 2005), but the contribution of each quadrant varies widely (Henry et al., 2004). While all quadrants contribute to the apical organ of the mollusc veliger (Hejnol et al., 2007), annelid trochophores (Lacalli, 1981) and the nemertean pilidium (Henry and Martindale, 1998; Martindale and Henry, 1995) and planuliform larvae (Maslakova et al., 2004b), only 1a and 1c form the apical organ of the polyclad Müller's larva (Boyer et al., 1998) and 1c and 1d give rise to the apical organ of a polyplacophoran mollusc (Henry et al., 2004). This comparative data suggests the apical organ of different spiralians have a variable embryonic origin, and that apical fates have shifted during spiralian evolution despite the conservative cleavage pattern. Therefore, the lack of 1b contribution in the apical organ of *M. membranacea* is likely lineage specific and unrelated to the evolution of the biradial cleavage pattern of bryozoans.

The animal blastomeres that give rise to the apical organ of *M. membranacea* cyphonautes larvae express the anterior markers *six3/6* and *dlx*. In both the bryozoan *M. membranacea* and the mollusc *Kelletia kelletii* (Lee and Jacobs, 1999), *dlx* is restricted to the animal blastomeres, suggesting that *dlx* might be involved in the patterning of animal-vegetal identities of these embryos. On subsequent stages *dlx* is associated to the development of the apical organ of the bryozoan larva. The gene *six3/6* is expressed in a broad apical domain early in development and associated to neural progenitors and serotonergic neurons related to the apical organ in later stages of *M. membranacea*. This pattern matches that of other spiralian larvae such as brachiopods (Santagata et al., 2012), annelids (Marlow et al., 2014; Steinmetz et al., 2010), nemerteans (Hiebert and Maslakova, 2015a; Hiebert and Maslakova, 2015b; Martín-Durán et al., 2015) and molluscs (Perry et al., 2015). In fact, the anterior/aboral expression of *six3/6* is conserved throughout metazoans embryos (Sinigaglia et al., 2013) independent of the early cleavage pattern. Thus, what remains to be determined is the interplay between the molecular patterning and the cleavage pattern in driving the fates of embryonic blastomeres.

Ciliated band

Annelids, molluscs and nemerteans have a anterior ciliated band in their larval stages with a similar embryonic origin (Damen and Dictus, 1994; Henry et al., 2007; Maslakova et al., 2004a; Maslakova et al., 2004b). Such structure – the prototroch – is considered an ancestral trait for the trochozoan spiralians (Rouse, 1999). Our data reveals that the corona of the bryozoan *M. membranacea* and the primary trochoblasts of the mollusc *Patella vulgata* prototroch (Damen and Dictus, 1994) are formed by the equivalent blastomeres $1b_i$/$1b_e$ and $1b^1$/ $1b^2$, respectively. However, this similarity is restricted to the contribution of these early blastomeres. A more detailed analysis of their progeny reveals downstream differences between the cell lineages of the two ciliated bands (Figure S3). In addition, we found no evidence that the second quartet contributes to the corona of *M. membranacea* as observed in *P. vulgata* (Damen and Dictus, 1994). Despite the differences in the fate of the above blastomeres, our data on *otx* expression suggest these cells might share a similar molecular identity. In molluscs (Nederbragt et al., 2002a) and annelids (Arendt et al., 2001; Steinmetz et al., 2010) the expression of *otx* consists of an anterior ring associated with the developing prototroch. We find a similar ring of *otx2* expression in the bryozoan *M. membranacea* localized in the animal blastomeres $1b^1$ and $1b^2$, and also in the second and third quartet derivatives, cells that do not become part of the corona. Therefore, the expression of *otx* in an anterior ring might be conserved among spiralian embryos. Our combined gene expression and cell lineage data suggests that not all *otx*-expressing cells become ciliated cells. Thus, further experiments are needed to investigate the involvement *otx* in the patterning of these spiralian ciliated bands.

Blastopore

In most gymnolaemate bryozoans the blastopore closes after gastrulation (Pace, 1906; Prouho, 1892) or is not formed (Calvet, 1900) and its association to the larval mouth is still an open matter (Gruhl, 2009; Marcus, 1938; Prouho, 1892; Zimmer, 1997). Based on ultrastructural sections, Gruhl (2009) observed that the blastopore of *M. membranacea* persists until the formation of the larval mouth. Consistent with this finding, we show that the anterior border of the blastopore gives rise to the preoral funnel of *M. membranacea*, and that the endodermal cells lining the blastopore form the anterior portion of the larval gut. We also found *nk2.1* transcripts bordering the anterior lip of the blastopore and the anterior portion of the preoral funnel, and *foxa* expression surrounding the blastopore and larval mouth. These expression patterns indicate the molecular identity of the blastoporal lip of *M. membranacea* is associated to anterior and foregut fates. Thus, independent histological, molecular and cell lineage data provides robust evidence for a persistent blastopore and protostomic development in *M. membranacea*, as previously suggested (Gruhl, 2009).

Mesoderm

The source of the bryozoan mesoderm remains a contentious topic (Gruhl, 2009). Classical works suggest that mesodermal cells derive from endodermal blastomeres, but could not demonstrate the embryonic origin with cellular resolution (Barrois, 1877; Calvet, 1900; Corrêa, 1948; d'Hondt, 1983; Pace, 1906; Prouho, 1892). Recent ultrastructural data suggest a different hypothesis, that the mesoderm of the bryozoan *M. membranacea* originates from the delamination of one ectodermal cell during gastrulation (Gruhl, 2009). Our cell lineage data indicate that the first mesodermal cells of *M. membranacea* derive from the fourth quartet (4a–4d). The lateral cells $4a^A$ and $4c^A$ form the anterior muscles of the cyphonautes larva while the progeny of $4b^1$ gives

rise to a stack of mesenchymal cells that express the anterior mesoderm marker *foxf*. We did not observe the delamination of an anterior ectodermal cell as suggested by Gruhl (2009), but cannot discard the existence of ectodermally-derived cells contributing to the mesoderm of *M. membranacea*. Our work corroborate previous classical studies of bryozoan embryology by revealing that the mesoderm of the bryozoan *M. membranacea* originates from multiple fourth quartet blastomeres.

The source of mesodermal tissues in spiral-cleaving embryos is extensively studied and discussed (Ackermann et al., 2005; Boyer et al., 1996; Boyer et al., 1998; Conklin, 1897; Gline et al., 2011; Hejnol, 2010; Hejnol et al., 2007; Henry and Martindale, 1998; Kozin et al., 2016; Lambert, 2008; Lartillot et al., 2002b; Lyons and Henry, 2014; Lyons et al., 2012; Meyer et al., 2010; Render, 1997). There are generally two sources, an anterior mesoderm derived from the third quartet (ectomesoderm) and a posterior mesoderm derived from the 4d blastomere. Most spiralians have the 4d as the sole endomesodermal contributor, the annelid *Capitella teleta* is one exception (Eisig, 1898; Meyer et al., 2010), while the blastomeres contributing to the ectomesoderm are more variable (usually 3a and 3b) (Hejnol et al., 2007; Lyons and Henry, 2014), suggesting that the molecular underpinnings defining the fate of a cell can be coopted to different blastomeres (Hejnol et al., 2007). The source of mesodermal tissues of the bryozoan *M. membranacea* differs from other spiralians because (1) there is no contribution from the third quartet and (2) multiple blastomeres of the fourth quartet give rise to mesoderm. This suggests that the specification of the anterior mesoderm in the bryozoan might have been shifted in time and in position to the fourth quartet, being the most significant difference between the cell lineage of *M. membranacea* and spiral-cleaving embryos.

Descendants of the 4d cell form the germline and are known to express *nanos* in spiral-cleaving embryos (Rebscher, 2014). Germ cells have not been identified during the embryogenesis of any bryozoan and were only found in zooids after metamorphosis (Reed, 1991). We show that the germline marker *nanos* of *M. membranacea* is expressed in two posterior ectodermal cells at the 32-cell stage, and in two cells located in the internal sac in the late gastrula – presumably direct descendants of the early *nanos*-positive blastomeres. Since these blastomeres are not of endomesodermal origin and divide repeatedly during development, we hypothesize they might be stem cells contributing to the differentiation of the internal sac, an epidermal structure that persists during metamorphosis and gives rise to the outer case of the zooid (Stricker, 1988). Further analysis in competent larvae and metamorphosed juveniles should clarify the fate and molecular identity these cells.

A modified spiral cleavage

Recent phylogenetic trees based on high-throughput transcriptomic data confidently place bryozoans in the Lophotrochoza (Laumer et al., 2015; Struck et al., 2014). This framework indicates that the spiral arrangement of blastomeres during embryogenesis is ancestral to the clade and likely modified within the bryozoan lineage. Our investigation shows several similarities between the embryonic development of the bryozoan *M. membranacea* and the embryogenesis of annelids, molluscs, nemerteans and polyclads. The vegetal blastomeres sequentially give rise to quartets of daughter cells, the first asynchronous cell divisions occur in the posterior quadrant, the quadrant identities can be identified at the 32-cell stage, the MAPK activity resembles that of equal-cleaving molluscs and several genes are expressed in equivalent blastomeres or embryonic positions. In addition, the early blastomeres of *M. membranacea* and of

spiral-cleaving embryos have correspondent fates in the larval tissues. That is, the first animal blastomeres form the whole region between the apical organ and ciliated band – equivalent to the pretroch region – the second and third quartets contribute to the oral/anal ectoderm and the fourth quartet gives rise to the mesoderm of the larva, while the four large vegetal blastomeres are internalized and become endoderm. Given the phylogenetic position of bryozoans, we interpret these similarities as inherited traits from an ancestral spiral-cleaving development.

In contrast, certain traits are unique to the bryozoan, such as the biradial cleavage pattern with animal octets and the multiple endomesodermal sources. Our analysis suggests that during the evolution of gymnolaemate bryozoans the ancestral spiral cleavage pattern, characterized by the alternating oblique cell divisions, was modified to a biradial cleavage pattern. Some aspects of the development have remained conserved, such as the D quadrant specification, MAPK activity and overall fate map, while the orientation of the mitotic spindles changed and deviations appeared in the specification of the anterior mesoderm and the downstream portions of the cell lineage. Such scenario assumes that the polyembryony and irregular cleavage of phylactolaemates and stenolaemates are a derived condition for Bryozoa. Nevertheless, the internal phylogeny of bryozoans is not yet sufficiently resolved (Waeschenbach et al., 2012) and further work is necessary to clarify if the biradial cleavage of gymnolaemates represents the ancestral condition for the group.

Other cases for the evolutionary modification of the spiral cleavage pattern occur within the flatworms and molluscs (Hejnol, 2010). In cephalopods, the embryonic development is modified to the extent that there are no traces of the ancestral spiral cleavage (discoidal cleavage) (Wadeson and Crawford, 2003), which can only be inferred by the phylogenetic position. In cases where remnants are observed, they relate to the oblique orientation of the mitotic spindles. An example is the flatworm *Macrostomum lignano* that displays a typical spiral cleavage pattern until the third cleavage, when the embryonic development becomes considerably modified (Willems et al., 2009). Therefore, the bryozoan *M. membranacea* differs from previously known cases because we have identified cell lineage and developmental traits shared with spiral-cleaving embryos that are not the cleavage geometry itself. The mechanisms for the proposed evolutionary shift remain unclear, but changes in the orientation of the mitotic spindle have a genetic basis and are beginning to be uncovered (Davison et al., 2016; Kuroda, 2015). Our work suggests that the quartet-divisions, cell fates and other traits commonly associated with a spiral cleavage program can, in fact, be maintained despite the evolutionary modification of the cleavage geometry.

Evolution of cleavage patterns

There is no conclusive explanation for the diversity (or conservation) of metazoan cleavage patterns (Valentine, 1997). It has been proposed that the fate of blastomeres during embryogenesis is causally associated to the originating cleavage pattern (Valentine, 1997; Wray, 1994). In this case, a change in the cleavage geometry is correlated with a change in the cell fates. However, the bryozoan cell lineage does not support the evolutionary coupling of cleavage pattern and blastomere fates. We find that the fate of the early blastomeres are conserved between *M. membranacea* and spiral-cleaving embryos despite the highly modified biradial cleavage pattern. The relative positioning of the second and third quartets even differ between the bryozoan and a typical spiral cleavage, but these blastomeres still give rise to similar tissues. A parallel case occurs in the nematodes where the cleavage pattern diverged dramatic

between the groups without a corresponding change in the phenotype (Schulze and Schierenberg, 2011). Our work suggests that the specification of the fates of the early blastomeres in spiralians is independent of the cleavage pattern.

We found several developmental genes expressed in a similar spatial arrangement between bryozoans and other spiralians. This molecular map is similar not only to the typical spiral-cleaving embryos, but also to brachiopod embryos, whose embryos have a much greater number of cells and no stereotypic cleavage pattern (Long and Stricker, 1991). Thus, a single cell in the bryozoan embryo expressing *gata456* (Figure 10) might correspond to a whole region of *gata456* expression in the brachiopod embryo (Passamaneck et al., 2015), as suggested by Hejnol (2010). This reinforces the hypothesis that cell determination is not tied to a particular cleavage pattern, but depending on the underlying molecular framework established early in development (Henry et al., 1992). Our findings indicate that in evolutionary terms, the causal ontogenetic connection between cleavage pattern and blastomere fates, if any, can be broken (Scholtz, 2005). Further comparative cell lineage studies with other non-spiral spiralian lineages, such as gastrotrichs and rotifers, will be crucial to establish the ancestral traits of spiralian development and to better comprehend the relation between cleavage patterns and cell fates during evolution.

Conclusions

The embryonic development of *M. membranacea* provides a unique comparative standpoint to the typical spiral cleavage pattern. It reveals that spiral cleavage is not an all-or-nothing character and has been extensively modified in the diverse spiralian lineages. In particular, we suggest that the cleavage geometry of the bryozoan embryo evolved decoupled from other spiralian developmental traits. Therefore, modifying spiral cleavage does not require drastic developmental changes such as the ones found in cephalopods or parasitic flatworms. Furthermore, our work alleviates the idea that the cleavage pattern is evolutionary coupled to the specification of cell fates (Wray, 1994). In this perspective, the evolutionary conservation of cell fates in spiral cleavage, might be a consequence of a conserved underlying molecular patterning – the main driver of cell fates – overlaid by a stereotypic cleavage pattern.

Methods

Collection, spawning and cultures

We collected *M. membranacea* in the fjord waters of Hjellestadosen (60°15'23.9"N 5°14'20.1"E) in Bergen, Norway, between May and September. We handpicked kelp blades with ripe bryozoan colonies from floating boat docks, and maintained the leaves in tanks with flowing sea water at 10°C. To induce spawning, we cut a portion of the kelp blade with mature colonies, usually the ones with more opaque whitish/pinkish zooids, and transferred it to glass bowl with sea water sterilized with UV-light and filtered through a 0.2µm mesh (UVFSW). The bowl was placed under a stereomiscroscope with direct light and a digital thermometer to monitor the water temperature. Ripe colonies begin to spawn in around five minutes or more, or usually when the temperature reached 15°C. Once the temperature raised to 16 °C, the bowl was cooled down on ice with no direct light. The spawning colony was sequentially transferred to new bowls with UVFSW at 10°C to distribute the vast amounts of eggs. For each bowl with eggs, we added EDTA to a final volume of 0.1mM (usually

~20µL of 0.5M EDTA) to induce egg activation (Reed, 1987). The bowl was then placed in a incubator at 15°C for 30–60 min. Activated eggs were concentrated by swirling, distributed to smaller glass bowls with UVFSW and washed twice to remove the EDTA. We adjusted the amount of eggs per bowl to avoid that the eggs sitting on the bottom of the dish touch each other. We kept the cultures at 15°C. One colony could be re-used for spawning multiple times. *M. membranacea* colonies maintained in the flowing tanks remained viable to developmental studies for a week.

4D recordings and cell tracing

We pipetted embryos at the 2-cell stage to a glass slide coated with poly-l-lysine. We mounted the embryos under a cover slip with supporting clay feet, completed the volume with UVFSW and sealed the cover slip with vaseline. The slide was put under the 4D microscope (Hejnol and Schnabel, 2006) with a cooling ring around the objective to keep the temperature at 15°C. We recorded full-embryo stacks (40–60 optical slices) every 40s under differential interference contrast. Development was recorded for approximately 24h, when the embryo became ciliated and swam away from the field of view.

Raw data consists of a sequence focal levels for each time point. We loaded the data into the tracking software SIMI°BIOCELL (SIMI®) and manually traced individual cells. The results of this manuscript are compiled from the cell tracking data of four different embryos (Figure S4). Source files are available at 10.6084/m9.figshare.3569691.v1.

Cell lineage nomenclature

To analyze and compare the cell lineage of *M. membranacea* we annotated the individual cells with a modified spiral cleavage nomenclature (Child, 1900; Conklin, 1897; Wilson, 1892). The identical blastomeres at the 4-cell stage were labeled as A, B, C and D according to their correspondent fate, as identified by the video recordings. In such case, the D quadrant was assumed to be the blastomere giving origin to the dorsal/posterior region of the cyphonautes larva. At the 8-cell stage, the animal blastomeres were named 1a–1d and the vegetal blastomeres 1A–1D. The first cleavage of these animals blastomeres give rise to the first octet, referred with the subscript $_o$ (e.g. $1q_o$ refers to all cells of the first octet). An octet is made from four inner cells, indicated by the subscript $_i$ (for internal), and four outer cells indicated by the subscript $_e$ (for external). Derivatives of the animal octets received the standard superscripts of spiral cleavage with ^{1} for the apical progeny and ^{2} for the basal progeny (e.g. $1a_i^1$ refers to the inner A quadrant cell of the apical progeny from the first octet). The quartets derived from the four large blastomeres were labeled as in spiral cleavage (2q–4q). And the progeny of the first twelve-tet followed the spiral cleavage ^{1} and ^{2} superscripts. Finally, we labeled meridional with the superscript ^{R} for the cell to the right and ^{L} for the cell to the left, when viewed from the egg axis.

Fixation methods

We fixed representative developmental stages for antibody staining in 4% formaldehyde for 1h at room temperature, washed the embryos in PTw (1x PBS + 0.1% Tween-20) and stored (in PTw) at 4°C. For in situ hybridization, we fixed the samples in a solution of 4% formaldehyde / 0.2% glutaraldehyde solution to avoid tissue damage during the protocol. After 1h fixation at room temperature, we washed the

embryos in PTw, dehydrated through methanol series and kept the samples in 100% methanol at -20°C.

Gene cloning and in situ hybridization

We assembled the Illumina reads from *M. membranacea* (SRX1121923) with Trinity (Grabherr et al., 2011) and used known genes to identify putative orthologs in the transcriptome. We performed PCR gene specific primer pairs on cDNA synthesized with the SMARTer RACE cDNA Amplification kit (Clontech). Primers were designed with Primer3 (Untergasser et al., 2012). We synthesized antisense DIG-labeled riboprobes with MEGAscript kit (Ambion) and performed colorimetric *in situ* hybridization according to an established protocol (Martín-Durán et al., 2012).

Gene orthology

Orthology was assigned by aligning amino acid sequences of *M. membranacea* against annotated genes from diverse metazoans using MAFFT 7.215 (Katoh and Standley, 2013), retaining only informative portions of the alignment with GBlocks 0.91b with relaxed parameters (Talavera and Castresana, 2007) and running a Maximum Likelihood phylogenetic analysis with RAxML 8.1.17 (Stamatakis, 2014) using automatic model recognition and rapid bootstrap. Alignments were manually verified using UGENE (Okonechnikov et al., 2012). Resulting trees from the maximum likelihood analysis were rendered into cladograms using the ETE Toolkit (Huerta-Cepas et al., 2010) (Figure S5). Source files are available at 10.6084/m9.figshare.3569685.v1.

Immunohistochemistry and MAPK antibody

We permeabilized the embryos with several washes in PTx (1x PBS + 0.2% Triton X-100) for 2h and blocked with two washes of 1h in PTx + 0.1% BSA (Bovine Serum Albumin) succeeded by 1h incubation in PTx + 5% NGS (Normal Goat Serum). Samples were incubated with the primary antibody for the MAPK diphosphorylated ERK-1&2 (Sigma M9692-200UL) and stored overnight at 4°C on a nutator. We removed the MAPK antibody with three 5 min and four 30 min washes in PTx + 0.1% BSA, blocked in PTx + 5% NGS for 1h and incubated nutating overnight at 4°C with the secondary antibody Anti-Mouse-POD conjugate (Jackson) diluted 1:250. We removed the secondary antibody with three 5 min followed by several washes in PTx + 0.1% BSA for 2h. To amplify and develop the signal, we incubated the embryos for 3–5 min with the provided reagent solution and fluorochrome from TSA reagent kit Cy5 (Perkin Elmer). We stopped the reaction with two washes in a detergent solution (50% formamide, 2x SSC, 1% SDS) at 60°C, to reduce background, followed by PTw washes at room temperature. We stained nuclei by incubating permeabilized embryos in DAPI 1:500 or Sytox Green 1:1000 for 2h. Nuclei staining was combined with f-actin staining by the addition of BODIPY FL Phallacidin 5 U/mL previously evaporated to remove methanol.

Microscopy and image processing

We mounted in situ embryos in 70% glycerol in PTw. Embryos from antibody staining were mounted in 97% 2,2'-Thiodiethanol (Asadulina et al., 2012; Staudt et al., 2007), 80% Glycerol in PBS or SlowFade® Gold Antifade (ThermoFisher). We imaged the samples with a Zeiss AxioCam HRc mounted on a Zeiss Axioscope A1, using differential interference contrast technique (Nomarski) for in situ hybridizations and a fluorescent lamp for the MAPK antibody staining. We used a Confocal Leica TCS SP5 to image fluorescent samples. Colorimetric in situ hybridizations were also

scanned under the confocal using reflection microscopy (Jékely and Arendt, 2007). We processed all resulting confocal stacks in Fiji (Schindelin et al., 2012). When necessary, we adjusted the distribution of intensity levels to improve contrast with Fiji or GIMP. We created vector graphics and assembled the figure plates using Inkscape.

Acknowledgements

We thank Anette Elde, Jonas Bengtsen and Anlaug Boddington for helping with the collections and Sabrina Schiemann for the help with 4D microscopy. The study was funded by the core budget of the Sars Centre.

Figures

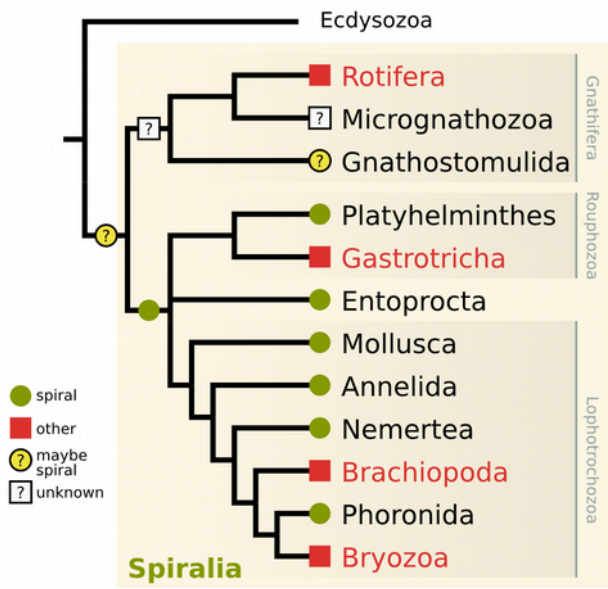

Figure 1. Phylogenetic distribution of the arrangement of embryonic blastomeres in Spiralia. Mapping refers only to the spiral symmetry as a result of the alternating oblique cell divisions, and not to other spiral cleavage traits (e.g. 4d mesoderm). Spiral symmetry is likely ancestral to the clade formed by Rouphozoa and Lophotrochozoa. Ancestral condition for Gnathifera and Spiralia remain less clear. Data from (Hejnol, 2010).

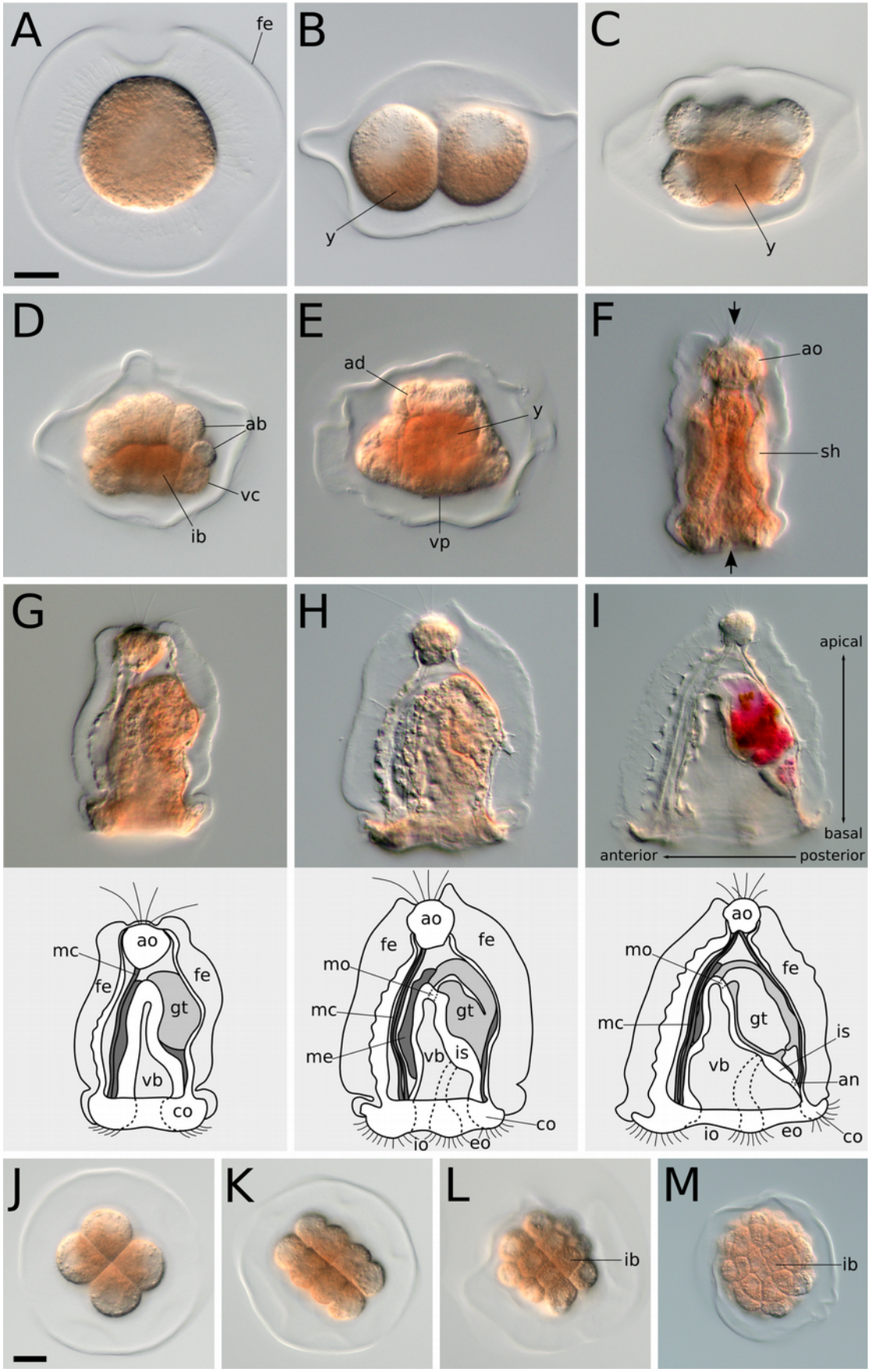

Figure 2. Overview of *M. membranacea* development. (A) Vegetal view of an activated egg becoming spherical. (B–I) Animal pole is top and vegetal pole is bottom. (B) 2-cell stage showing higher amount of yolk (y) on the vegetal side. (C) 8-cell

stage with yolk positioned on the inner cytoplasmic portions. (D) 28-cell stage. Large vegetal blastomeres carry most of the yolk with less yolk in the animal blastomeres (ab). (E) Anterior view of a mid-gastrula stage with a prominent apical disc (ad), vegetal ectoderm (ve) and an inner mass of yolk-rich blastomeres. (F) Frontal view of a late gastrula stage after the vegetal ectoderm invaginated and the embryo extended in the animal/vegetal axis. Most larval structures are formed by this stage, including the apical organ (ao) and shell valves (sh). At this stage, the cilia of the apical tuft and the corona breakthrough the fertilization envelope (arrows). (G–I) Lateral views showing the morphogenesis of the cyphonautes for 24h late gastrula (G), 48h larva (H) and 3d larva (I). Larval structures are illustrated below each panel. (J–M) Vegetal views showing beginning of gastrulation. (J) 8-cell stage. (K) 16-cell stage. (L) 28-cell stage. (M) 90-cell stage with vegetal blastomeres being internalized. co: corona, gt: gut, vb: vestibule, mc: muscle cell, me: mesodermal tissue, is: internal sac, mo: mouth, io: inhalant opening, eo: exhalant opening, an: anus. Scale bars = 20µm.

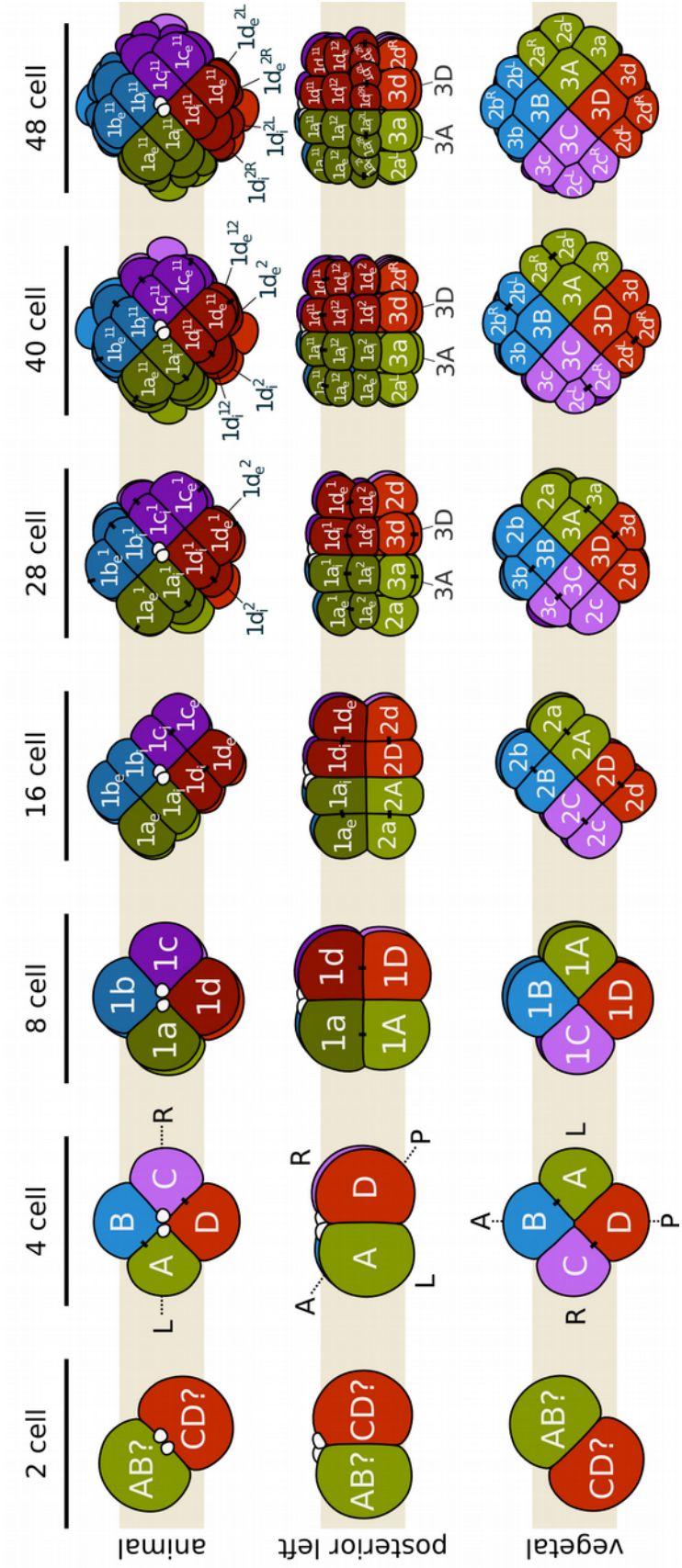

Figure 3. Cleavage pattern and orientation of the embryonic axes of *M. membranacea*. Quadrant identity was determined backwards from 4D microscopy recordings and it is not known if it is determined during early stages.

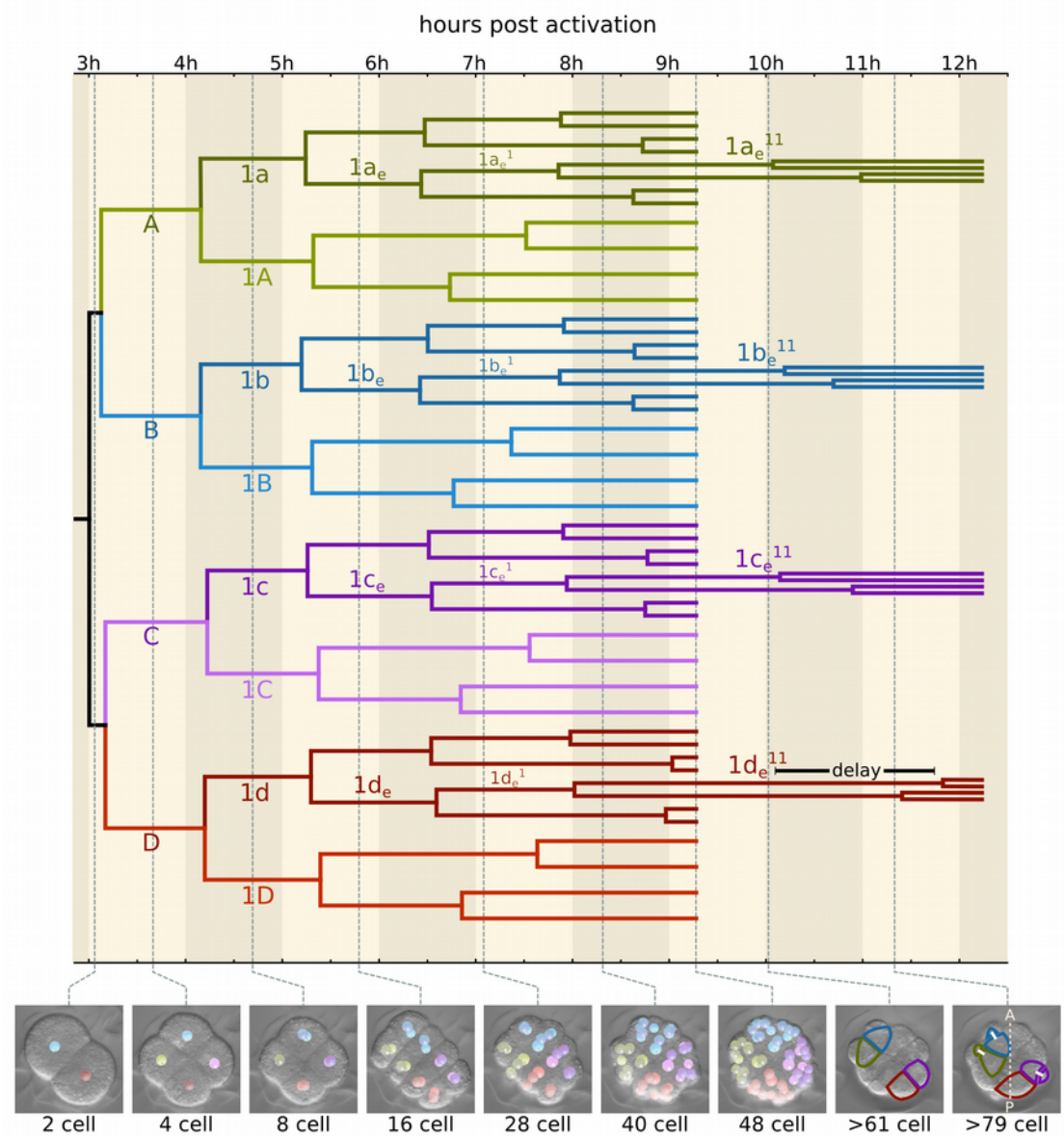

Figure 4. Timed cell lineage of *M. membranacea* and the break of biradial symmetry. Panels on the bottom show the developmental stages with the cell tracing overlay until the embryo with 48 cells. The outlines in the last two panels (>61 and >79 cells) indicate the cells $1a_e^{11}$–$1d_e^{11}$, and the prominent delay in the division of $1d_e^{11}$. The anteroposterior axis is denoted by a dashed line in the last panel. Quadrant color coding: A (green), B (blue), C (purple), D (red).

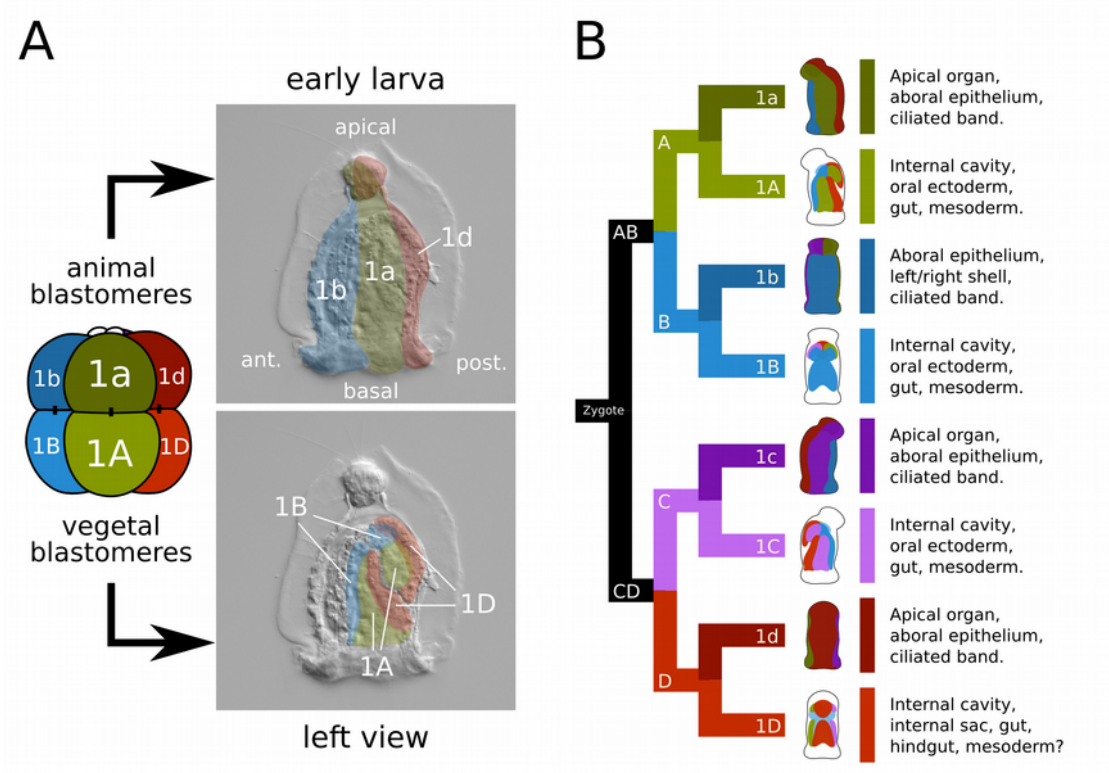

Figure 5. Larval fates of the eight embryonic blastomeres of *M. membranacea*. (A) Illustration based on the cell lineage data representing the overall fates of the animal (1a–1d) and vegetal (1A–1D) blastomeres. Animal blastomeres give rise to the apical organ, aboral epithelium and corona. Vegetal blastomeres give rise to the vestibule epithelium, oral ectoderm, mesoderm and gut. (B) Larval structures derived from each of the eight blastomeres. Quadrant color coding: A (green), B (blue), C (purple), D (red).

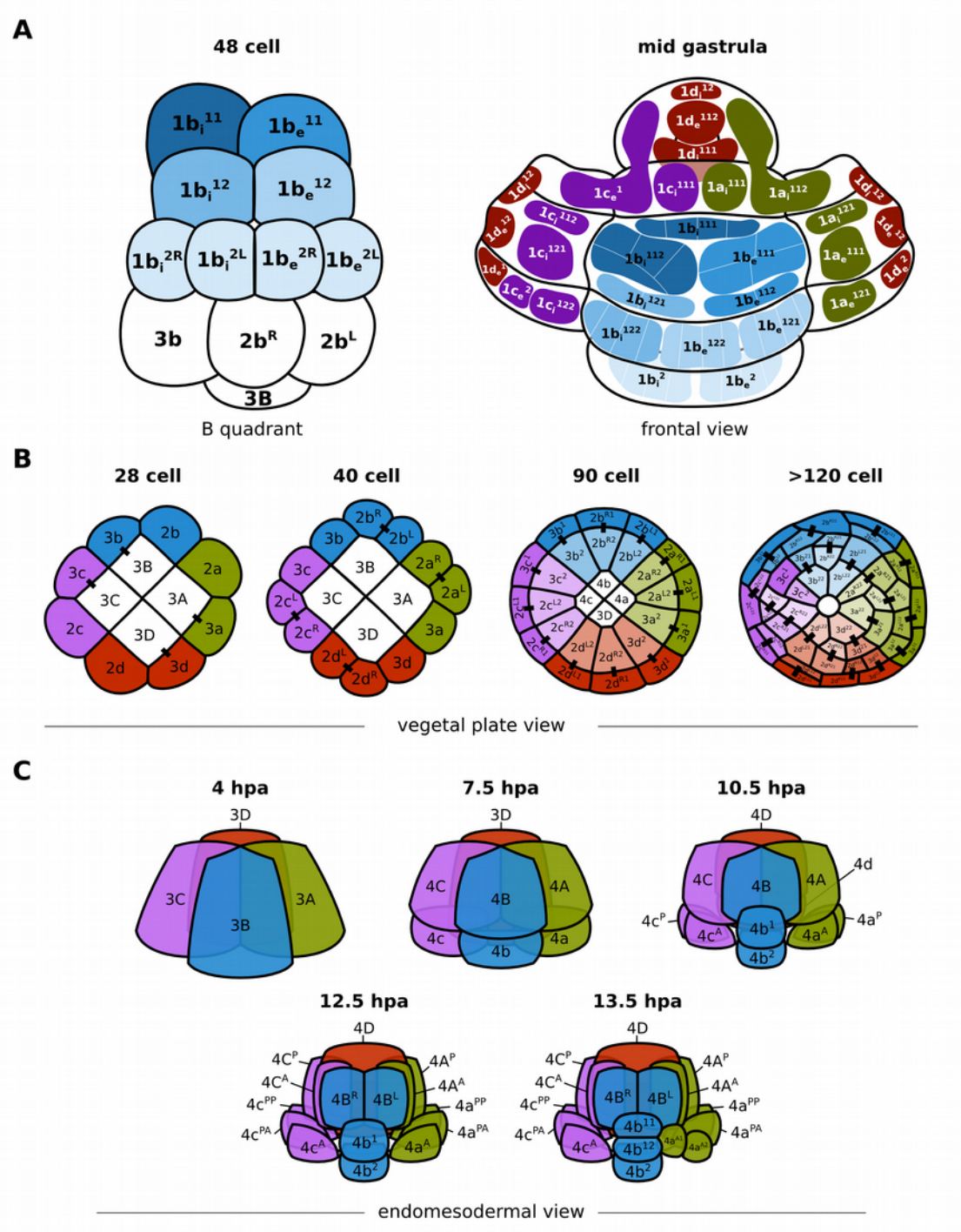

Figure 6. Details of the fate map and cleavage patterns of the animal blastomeres, vegetal ectoderm and internalized blastomeres of *M. membranacea*. (A) Representation of the B quadrant in frontal view at the 48-cell stage. Frontal view of the embryo at the mid gastrula stage with left, right and top regions "opened" for visualization. Shades of blue on the blastomeres of the 48-cell stage correspond to the fates in the epithelium and corona. White lines illustrate cell borders of further progeny from the blastomeres indicated. The fates of the blastomeres of other quadrants are indicated with the standard colors. (B) Cleavage patterns at the vegetal ectoderm. The original twelve-tet at the 40-cell stage divides once forming twelve derivatives, lining the forming blastopore at the 90-cell stage. At the subsequent division (>120 cells), progeny from the cells at the vertices ($2a^{L2}$, $2b^{R2}$, $2d^{R2}$ and $2c^{L2}$) disconnect from the blastopore lip. At this stage, only eight cells are lining the blastopore. The cell $3c^{1}$ and $3c^{2}$

do not divide. (C) Cleavage patterns of the four large blastomeres that internalize during gastrulation. Quadrant color coding: A (green), B (blue), C (purple), D (red).

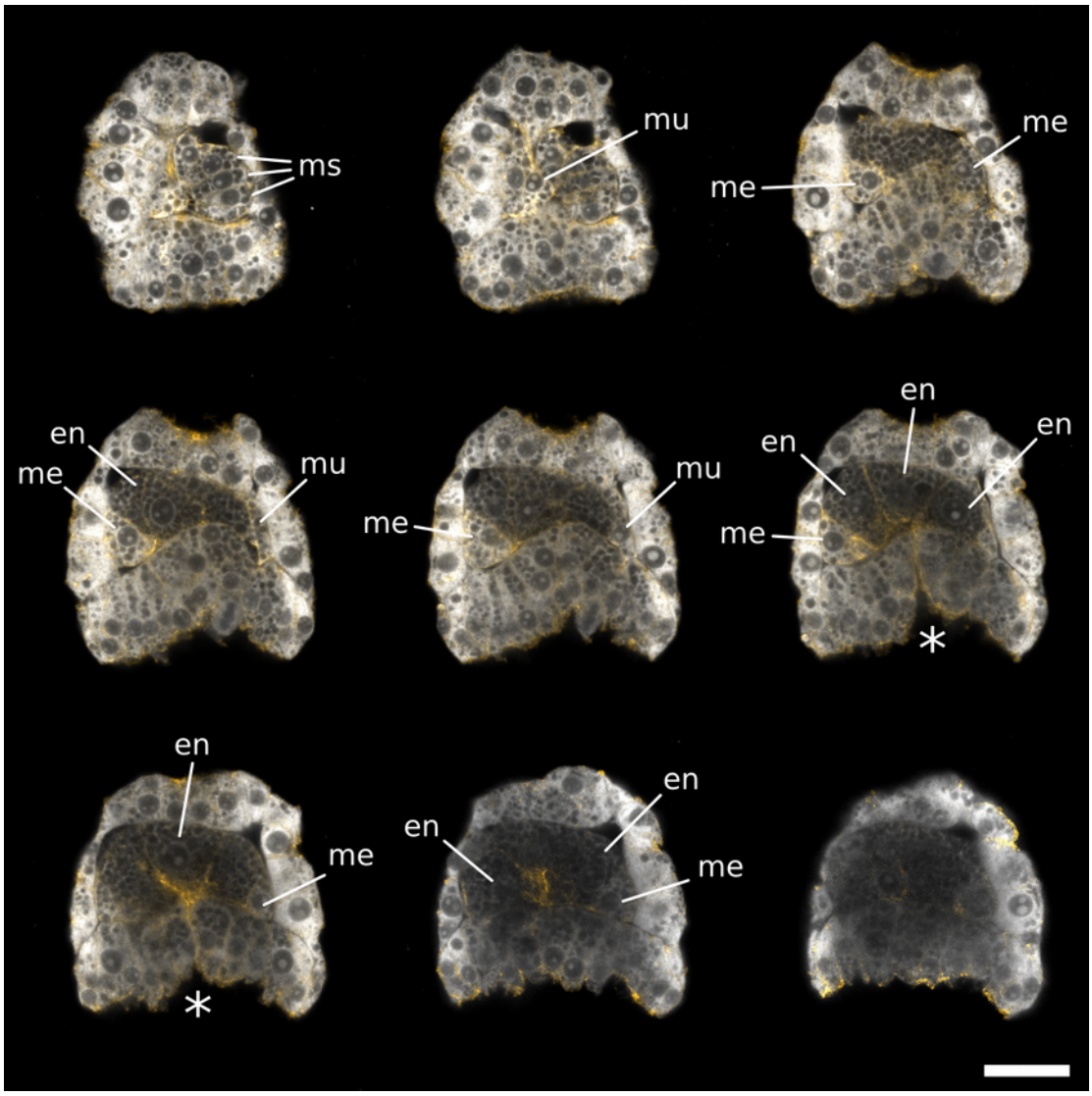

Figure 7. Mesodermal and endodermal cells in *M. membranacea*. Maximum intensity projections of 2–3 slices from a confocal stack at mid-gastrula stage. View of the anterior/right side of the embryo (top-left) to the posterior/left side (bottom-right). Samples stained with propidium iodide (grays) and phallacidin (orange). ms: mesodermal stack of cells from the B quadrant (4b derivatives), mu: muscle cells reaching the apical organ, me: other mesodermal cells, en: endodermal cells. Asterisk indicates the blastopore. Scale bar = 20µm.

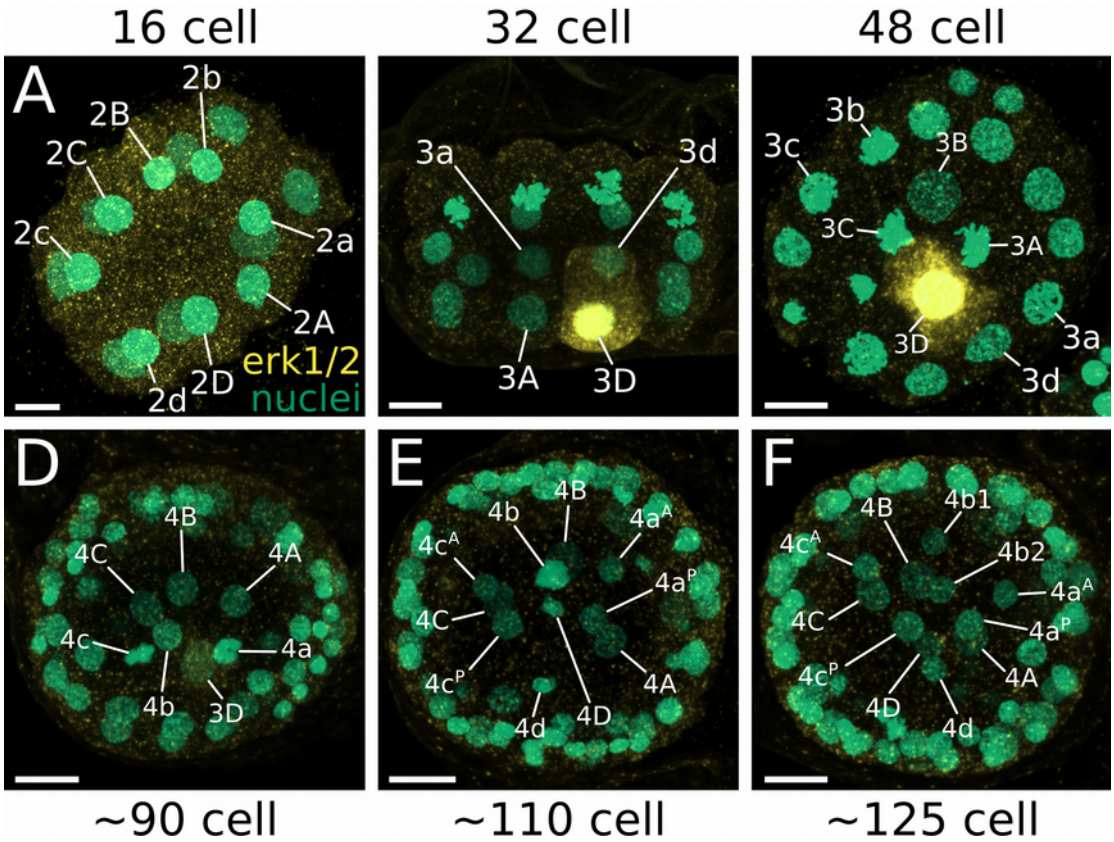

Figure 8. MAPK activity during the development of *M. membranacea*. (A) No detectable levels of activated MAPK at the 16-cell stage. (B) Side view showing only the quadrants A and D of a 32-cell stage with activated MAPK in the cell 3D. (C) Vegetal view of a 48-cell stage with blastomeres 3C and 3A undergoing mitosis. (D) Frontal view of an embryo with approximately 90 cells. 3D cell shows a weaker signal for MAPK activity. (E) Embryo soon after the division of the 3D cell. There are no detectable levels of MAPK activity in any cell. (F) Embryo with more than 125 cells without any detectable levels of MAPK activity. Scale bar = 10µm.

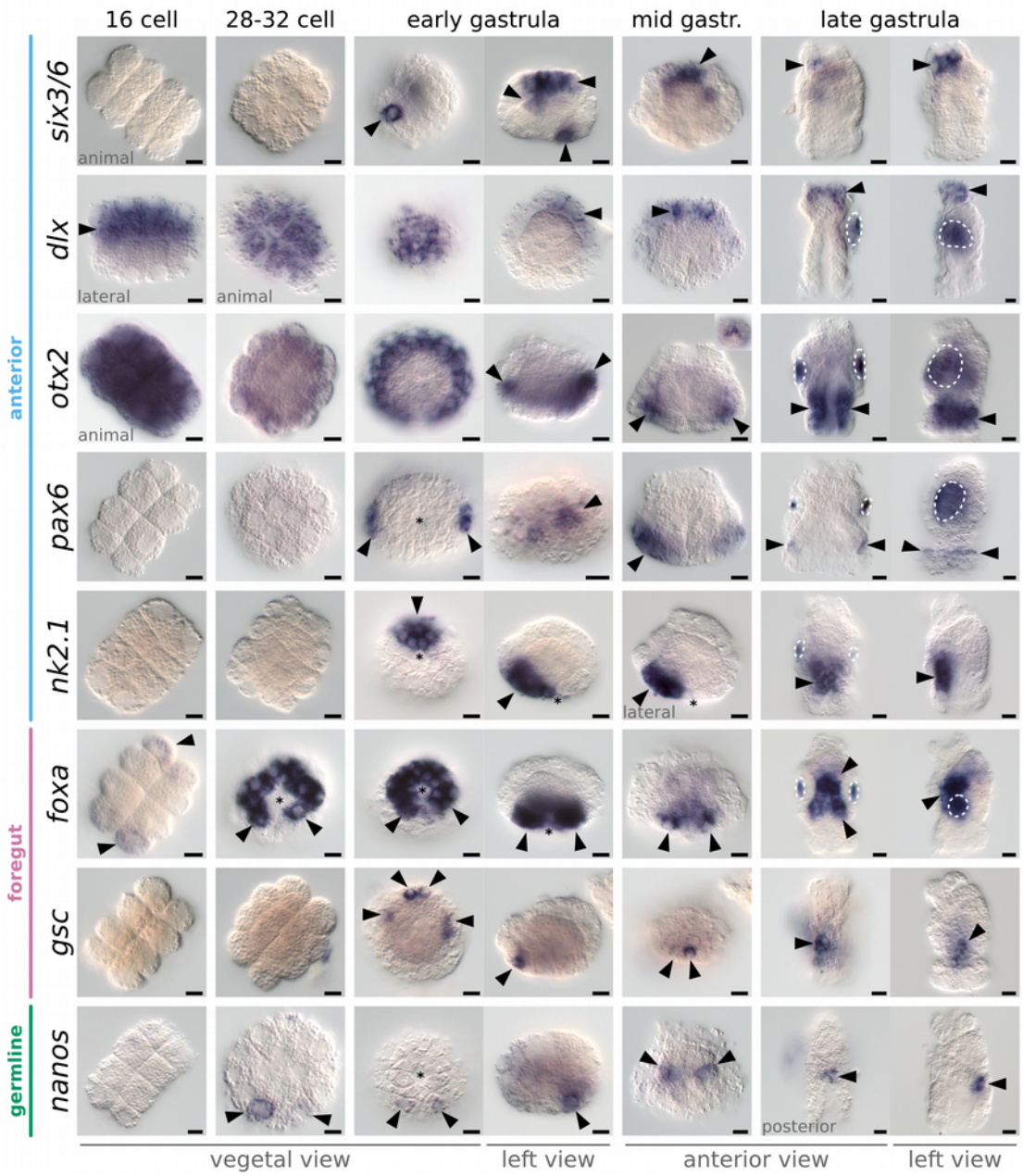

Figure 9. In situ hybridization of anterior, foregut and germline markers during *M. membranacea* embryonic development. Orientation of the embryos is listed below each column and exceptions are marked on individual panels. On vegetal views, B quadrant is top and D quadrant is bottom. On left views anterior (B quadrant) is to the left. All views, except vegetal view, the animal pole is top. Arrowheads indicate expression and dashed areas mark unspecific staining attached to the shell valves of some embryos. Asterisks indicate the position of the blastopore. Scale bar = 10µm.

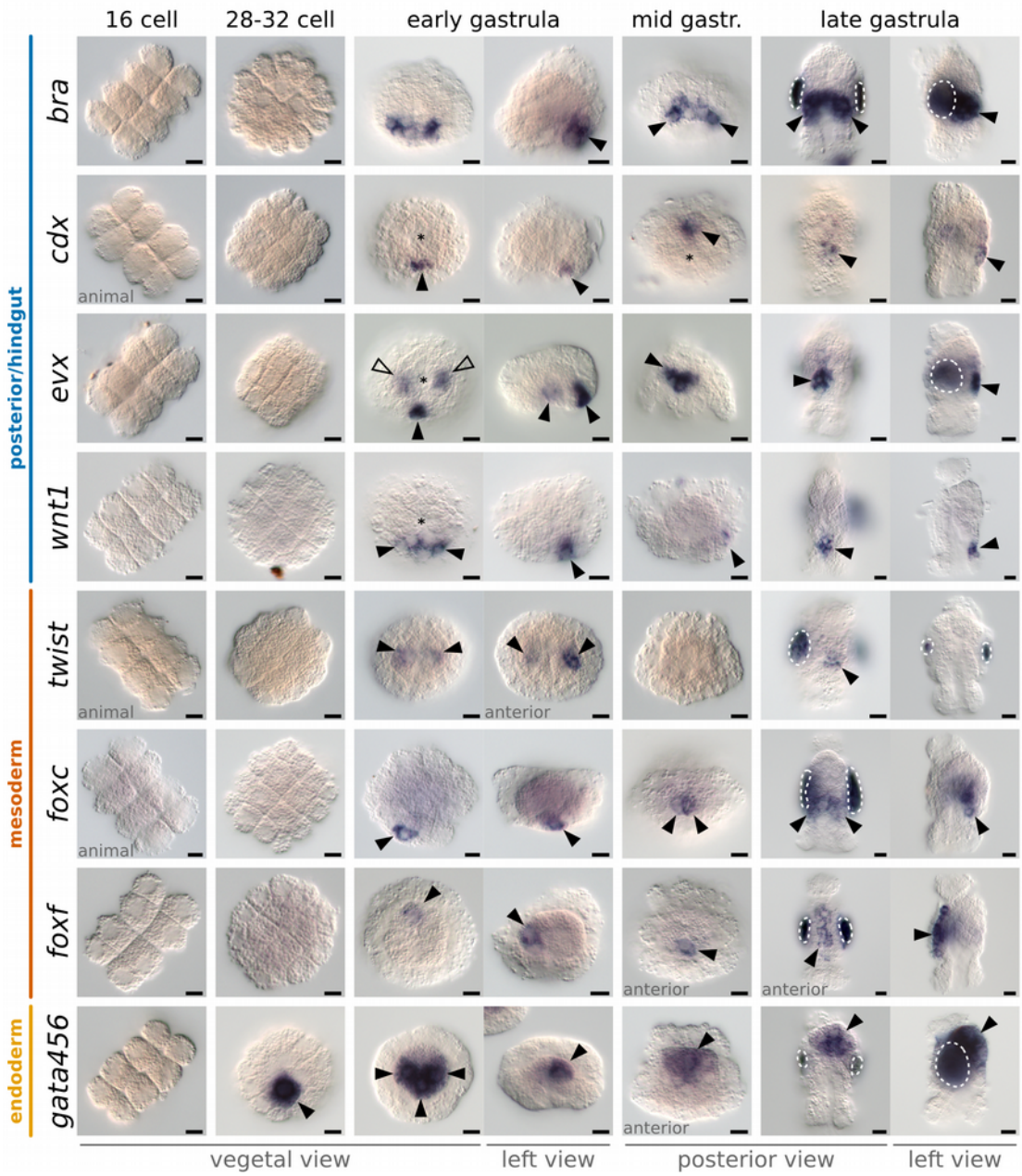

Figure 10. In situ hybridization of posterior/hindgut, mesoderm and endoderm markers in the development of *M. membranacea*. Orientation of the embryos is listed below each column and exceptions are marked on individual panels. On vegetal views, B quadrant is top and D quadrant is bottom. On left views anterior (B quadrant) is to the left. All views, except vegetal view, the animal pole is top. Arrowheads indicate expression and dashed areas mark unspecific staining attached to the shell valves of some embryos. Asterisks indicate the position of the blastopore. Scale bar = 10µm.

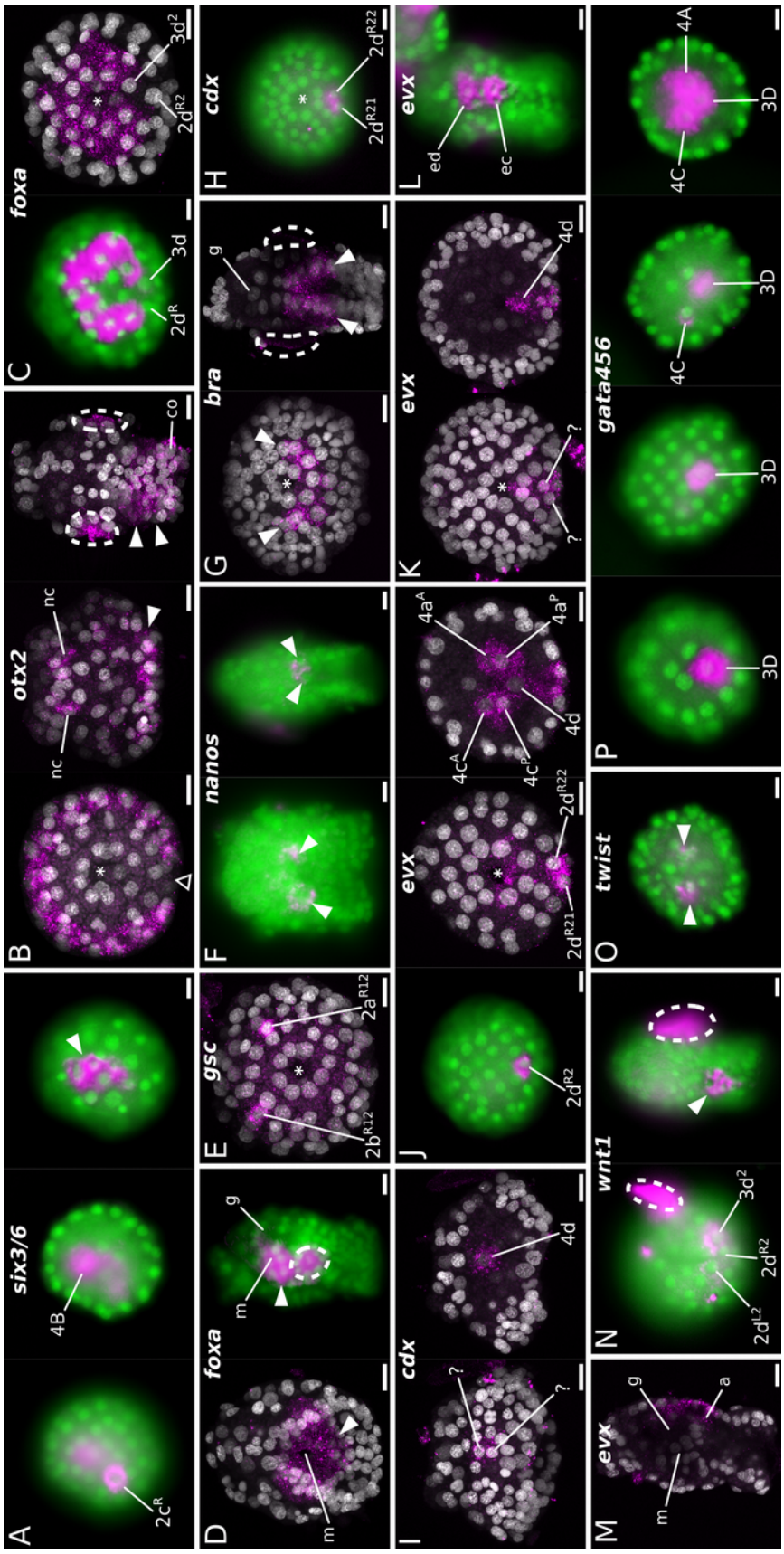

Figure 11. Gene expression details with cell resolution in *M. membranacea*. Selected embryos from the in situ hybridizations shown in Figure 9 and 10 observed under a fluorescent lamp (green=nuclei, magenta=signal) or maximum intensity projections from confocal microscopy (grey=nuclei magenta=signal). Arrowheads are pointing to

the relevant areas of gene expression while dashed areas mark unspecific background staining. Asterisks mark the position of the blastopore. (A) Expression of *six3/6* at different focal levels. (B) Expression of *otx2* in a vegetal view (left) showing the posterior gap in expression (triangle outline), neural cells at the apical disc (nc) of a mid-gastrula embryo and the wider expression in the late gastrula (arrowheads). (C) Expression of *foxa* at the 90-cell stage (left) without signal on the posterior cells $2d^{R}$ and 3d, and the same posterior gap one cell division cycle later (right). (D) Late gastrula stage (left) viewed from the posterior vegetal end to show the mouth opening with surrounding expression of *foxa* (B quadrant is bottom). On the right, a left side view with *foxa* expression in the mouth region. (E) Bilateral anterior cells expressing *gsc*. (F) Two *nanos*-positive cells during mid-gastrula (left) and late gastrula (right). (G) Posterior and lateral cells on the vegetal ectoderm expressing *bra* (left) and a posterior view of a late gastrula depicting the domain in the posterior epithelium of the vestibule (right). (H) Vegetal view of early gastrula with the two vegetal cells with *cdx* expression ($2d^{R21}$ and $2d^{R22}$). (I) *cdx* expression observed in two cells at the posterior ectoderm (left), and in the 4d cell (right) at mid-gastrula with two. (J) Expression of *evx* in one posterior ectodermal cell ($2d^{R2}$) on the vegetal side during early gastrulation (left). Progeny of $2d^{R2}$ expresses *evx* (center) as well as the derivatives of 4a and 4c and the 4d cell. (K) Mid-gastrula stage with *evx* expression in at least two posterior ectodermal cells (left) and in the 4d (right). (L) Posterior view of a late gastrula with *evx* expressed in the posterior endoderm (ed) and ectoderm (ec). (M) Left side view of *evx* expression at the late gastrula with posterior endodermal and ectodermal domains. (N) Expression of *wnt1* during early gastrulation is restricted to three cells, $2d^{L2}$, $2d^{R2}$ and $3d^{2}$ (left) and a posterior cluster of cells at the late gastrula (right). (O) *twist* expression in internalized blastomeres. (P) Expression of *gata456* from 32-cell stage until early gastrulation. Transcripts are restricted to the 3D until the internalization of vegetal blastomeres, when 4A and 4C initiate the expression of *gata456*. Scale bar = 10µm.

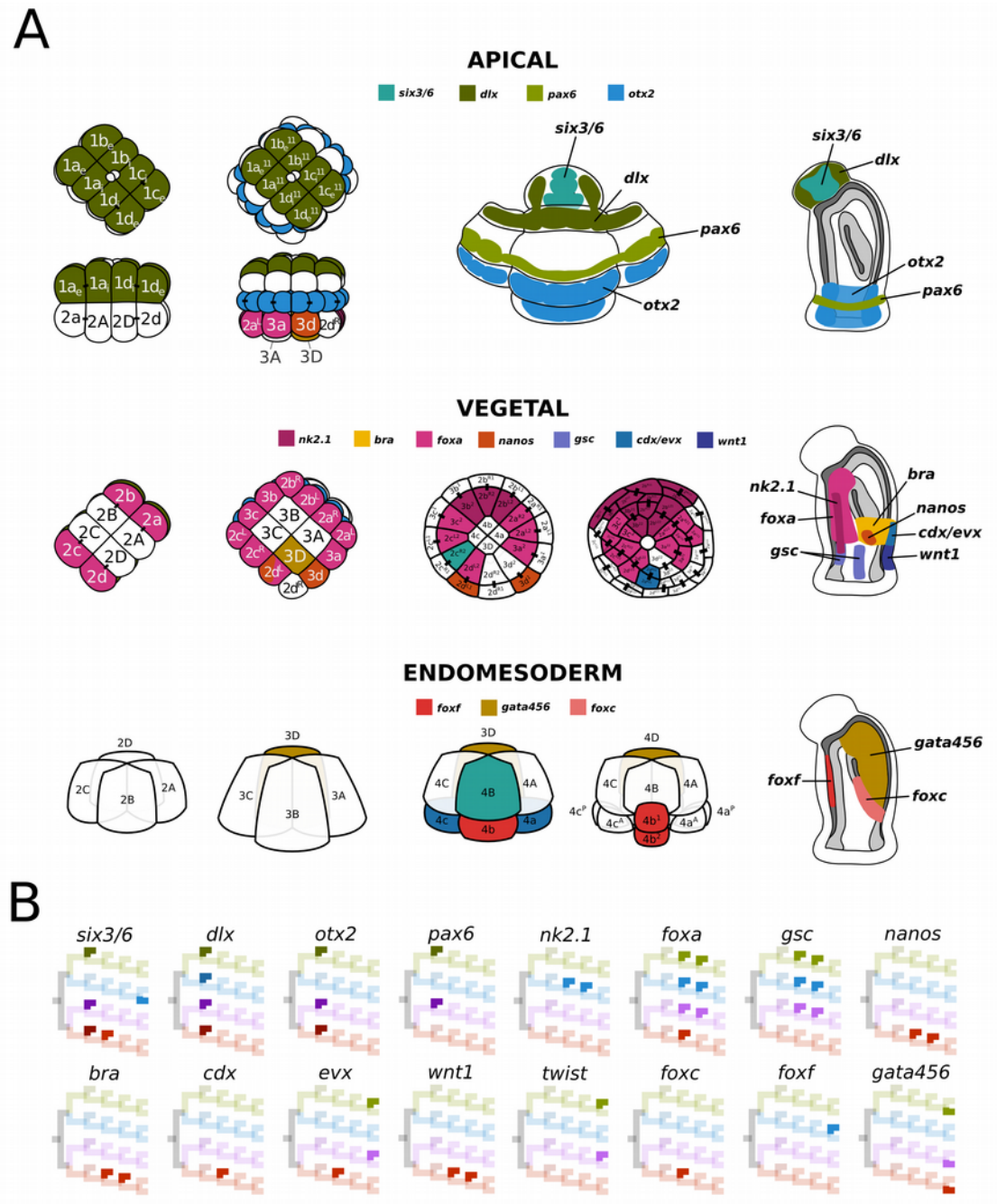

Figure 12. Gene expression throughout the cell lineage of *M. membranacea*. (A) Various developmental stages illustrating with cellular resolution, whenever possible, the expression of candidate genes in the animal ectoderm, vegetal ectoder and endomesoderm. (B) Cell lineage diagrams indicating in which lineages the genes are being expressed. Gene activity is indicated in the branches with vivid colors.

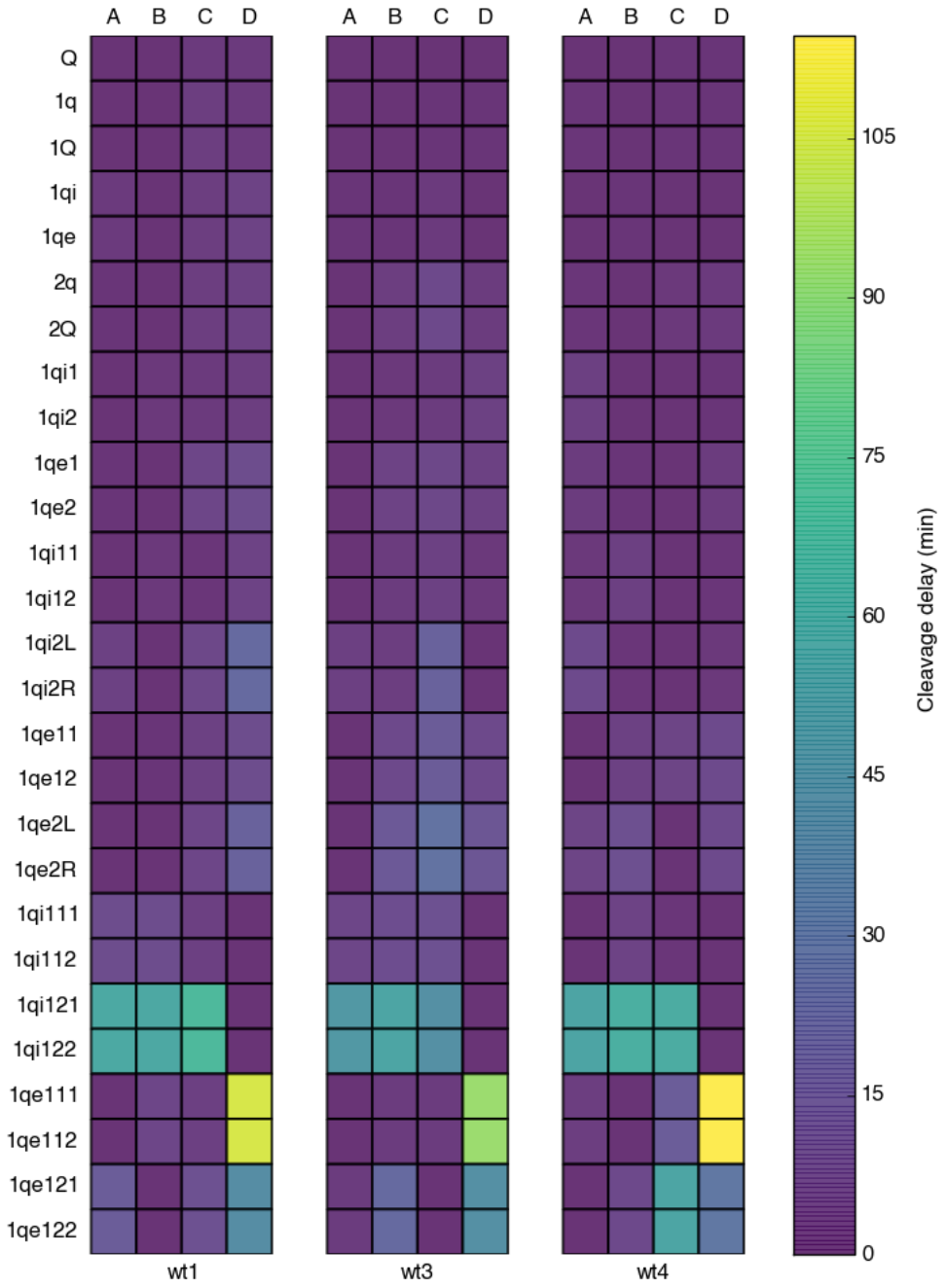

Figure S1. Synchrony in the cleavage of correspondent quartets in three *M. membranacea* embryos. The color gradient represents the time a cell took to divide after the first cell of its quartet had divided. Each column represents one embryo that has been tracked from the animal pole (wt1, wt3 and wt4). The most significant and consistent asynchronous events occur in the quartets $1q_i^{12}$ and $1q_e^{11}$.

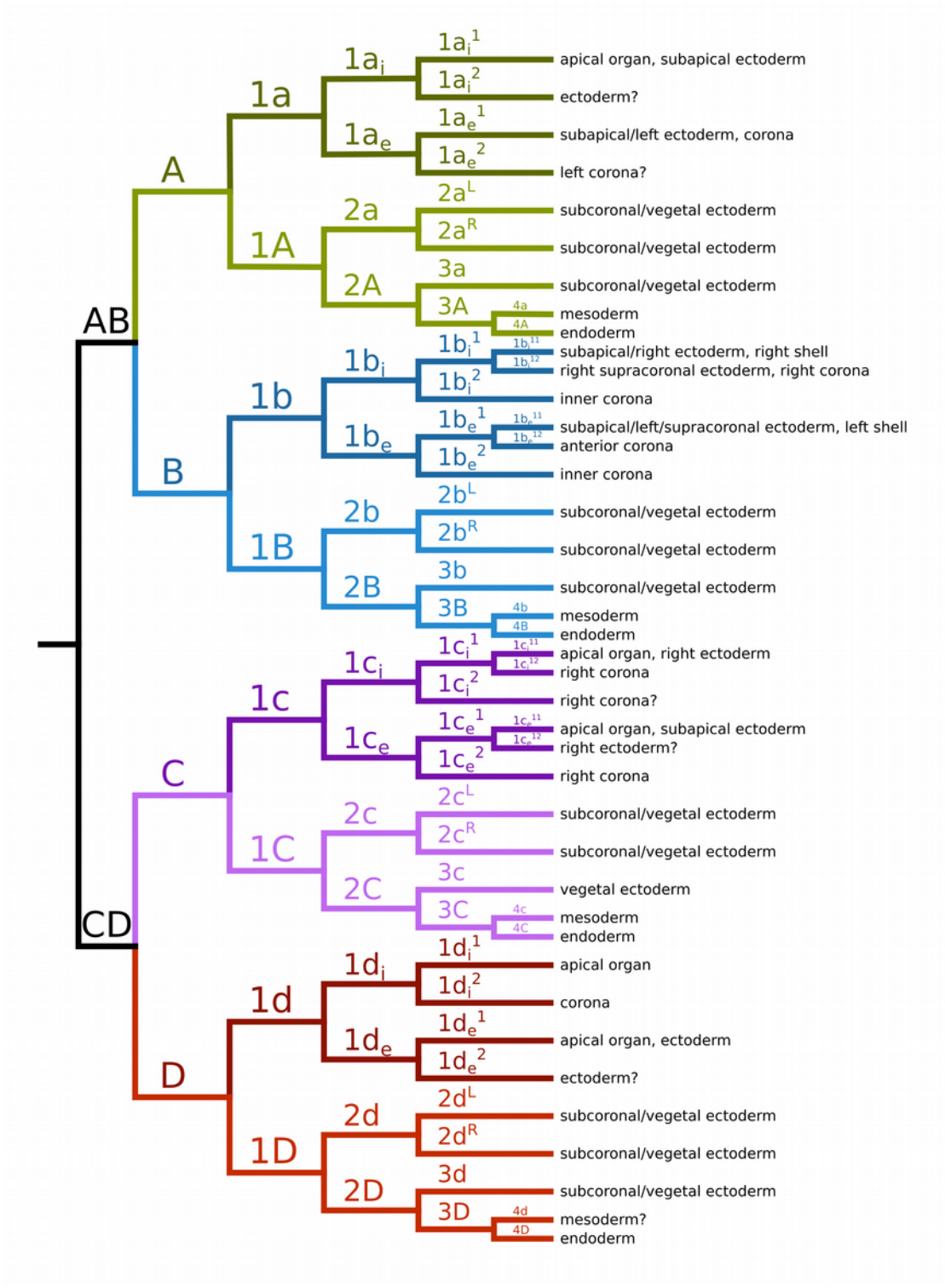

Figure S2. Detailed fate map of *M. membranacea*.

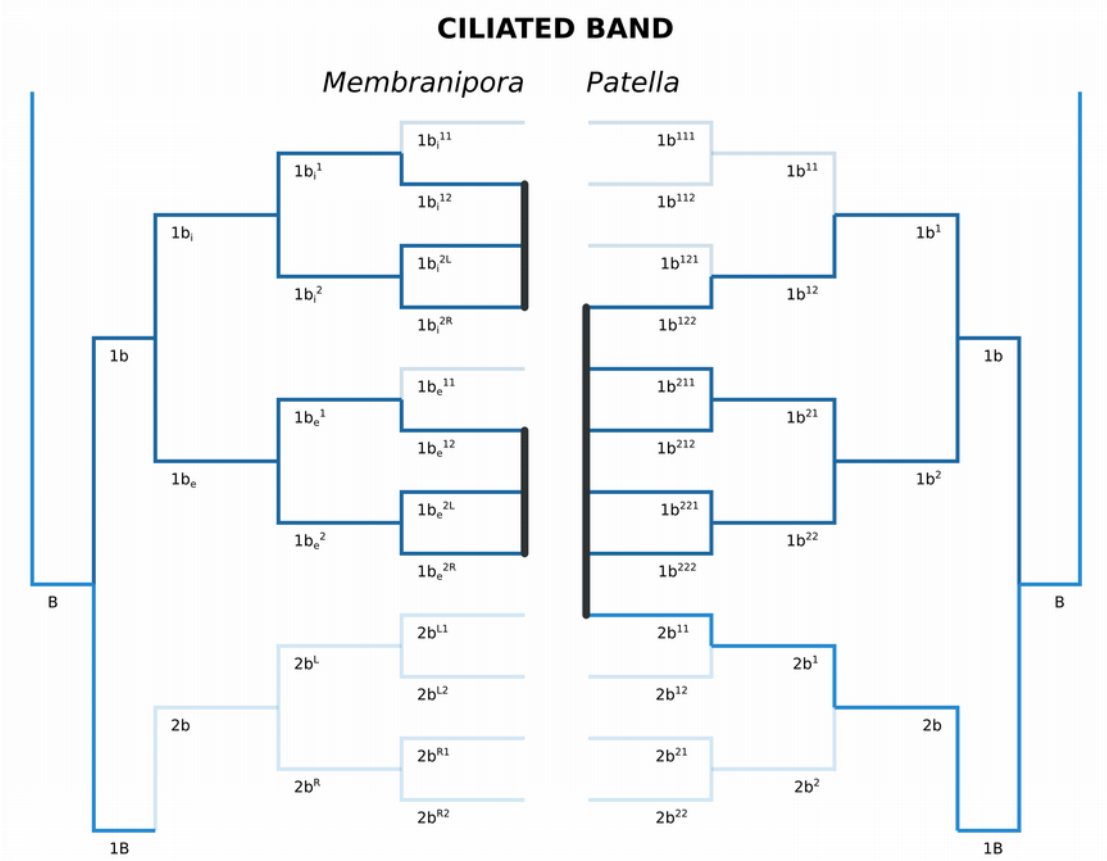

Figure S3. Cell lineage comparison between the larval ciliated bands of *M. membranacea* and *Patella vulgata* (Damen and Dictus, 1994).

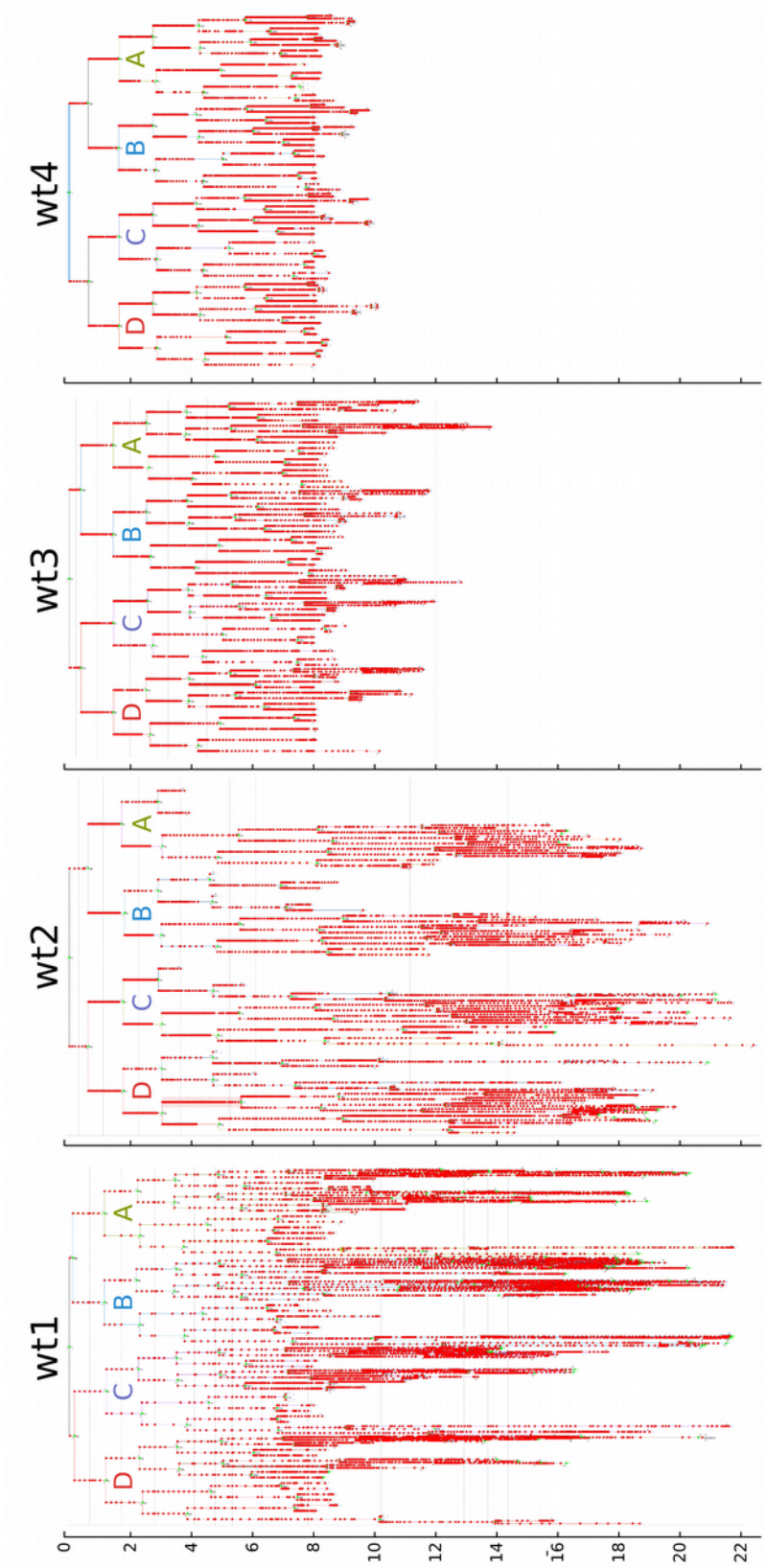

Figure S4. Cell lineages for three wild type (wt) embryos of *M. membranacea*. **wt1** is a recording of the animal pole providing most of the data for the aboral epithelium, **wt2** is a vegetal pole view providing detailed information for the vegetal ectoderm, and **wt3** and **wt4** are additional recordings of the animal pole. Development time measured in hours post activation (hpa) is shown in the Y axis.

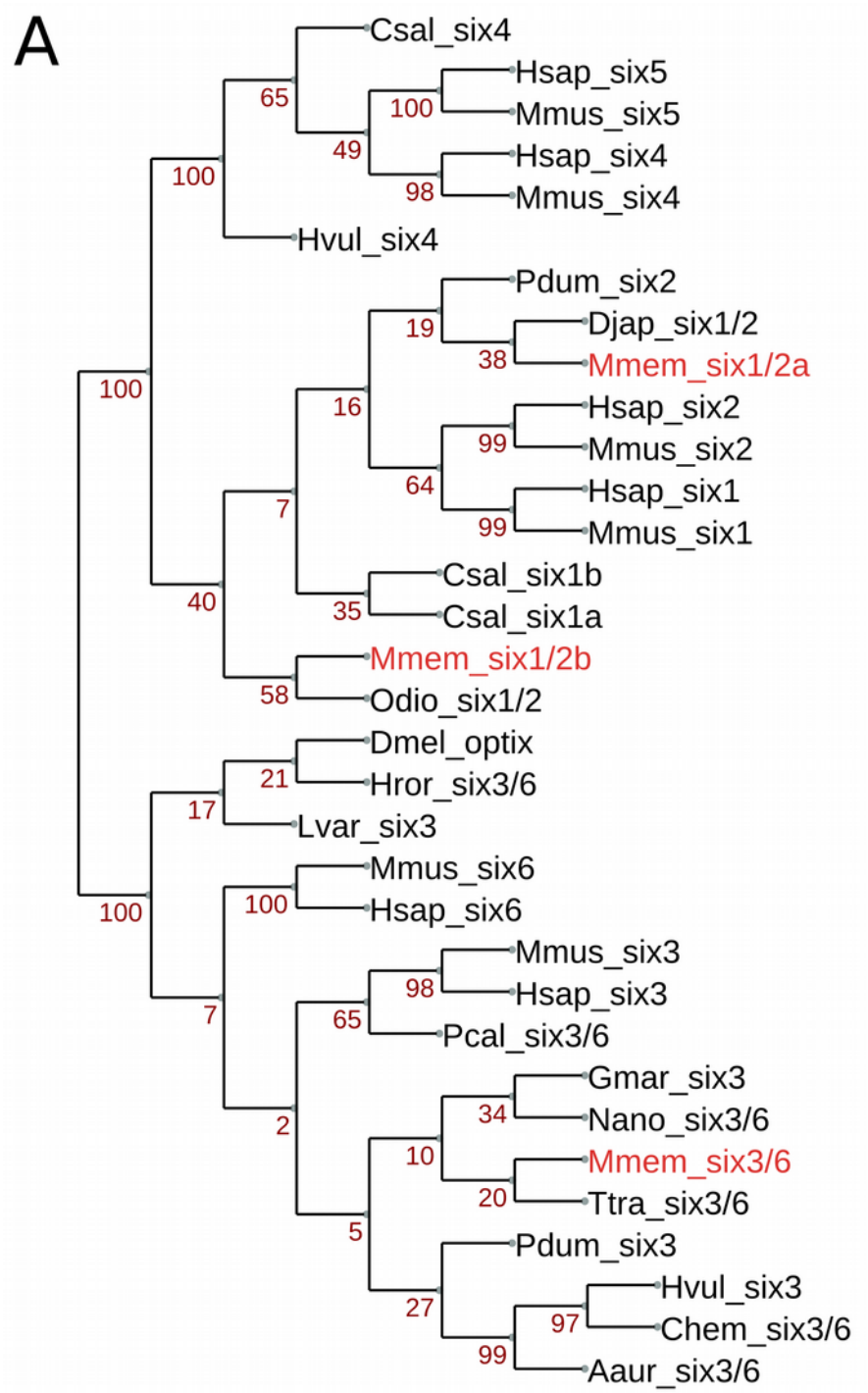

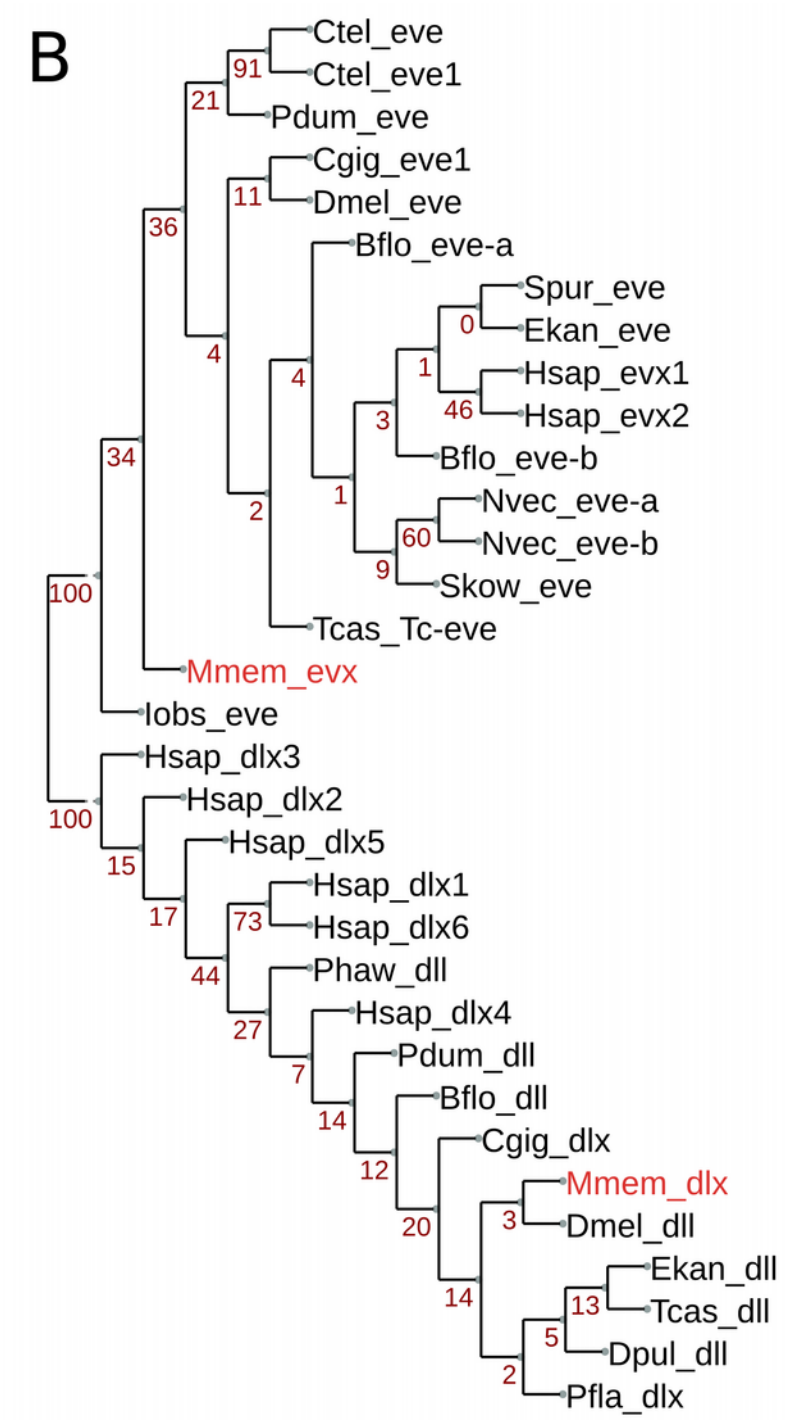

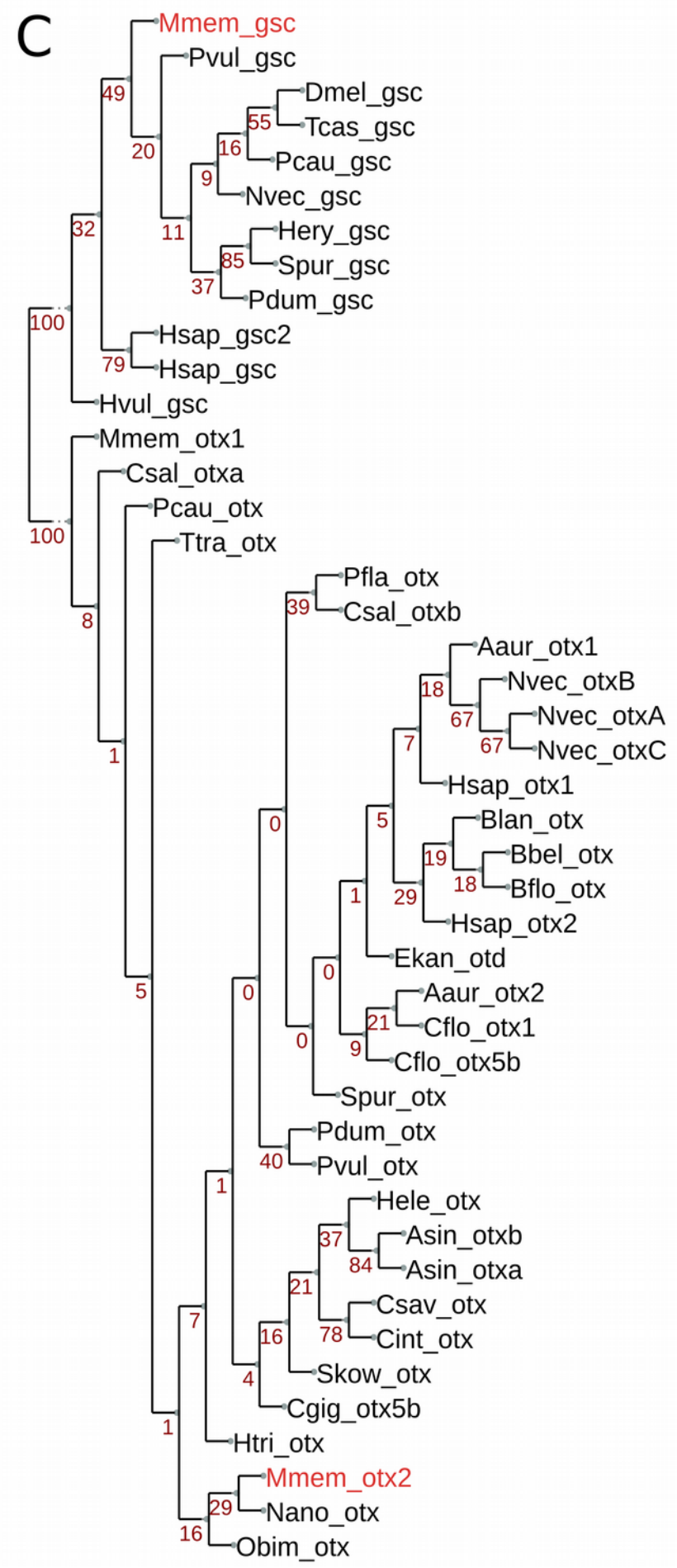

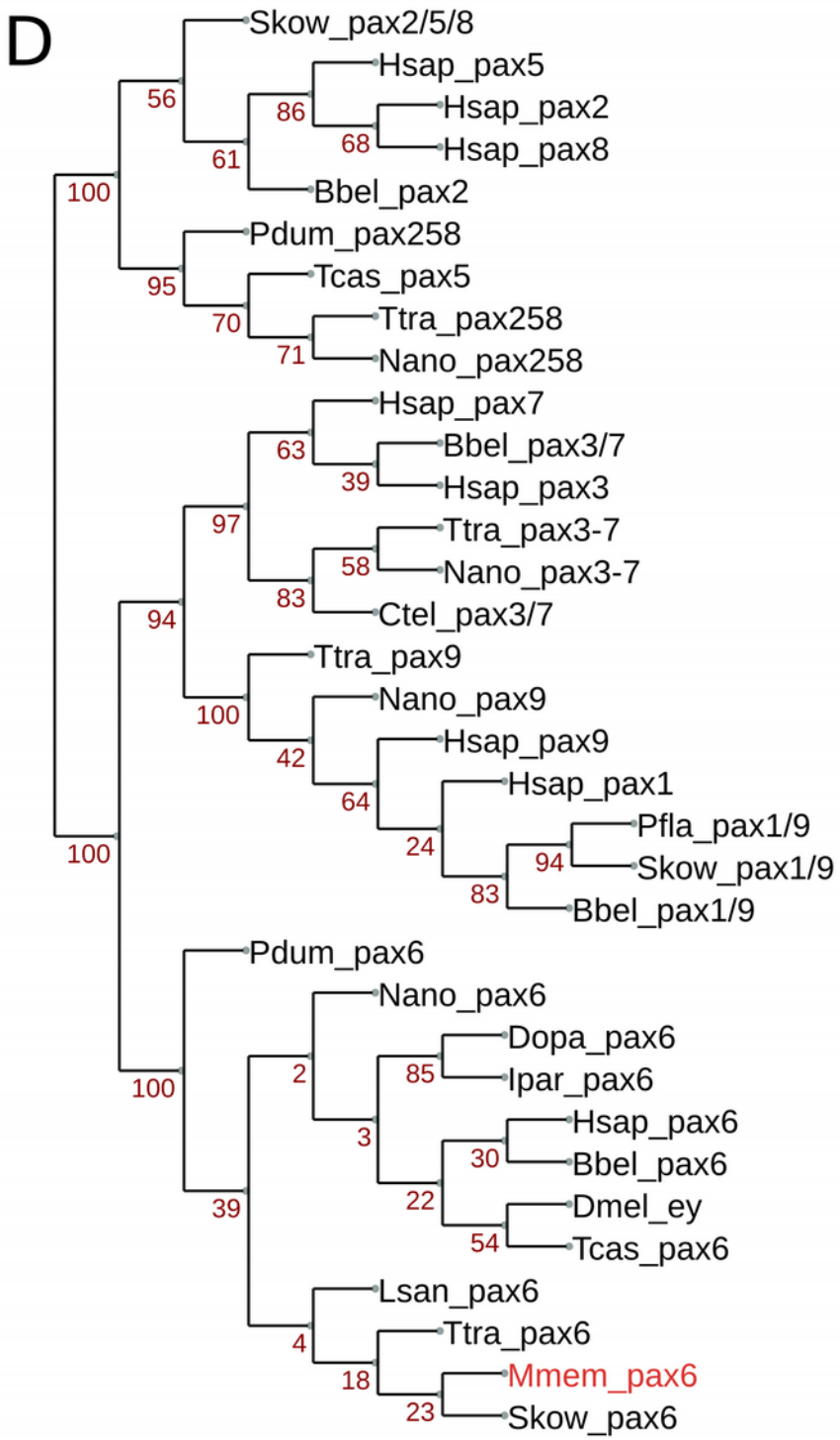

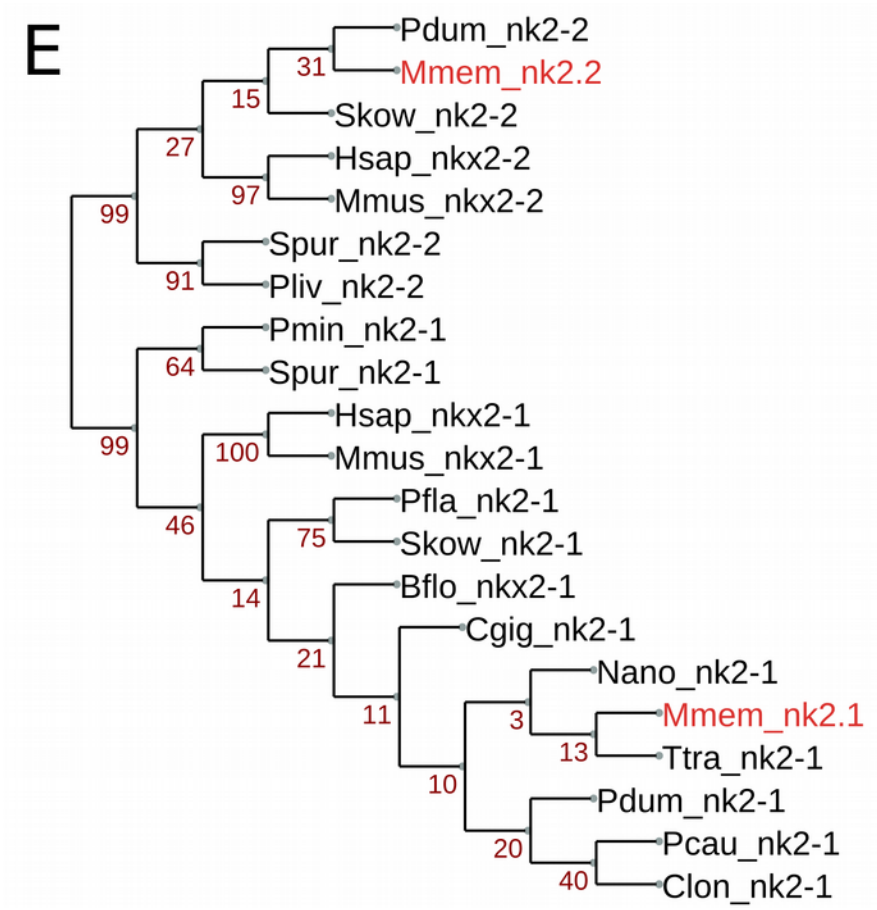

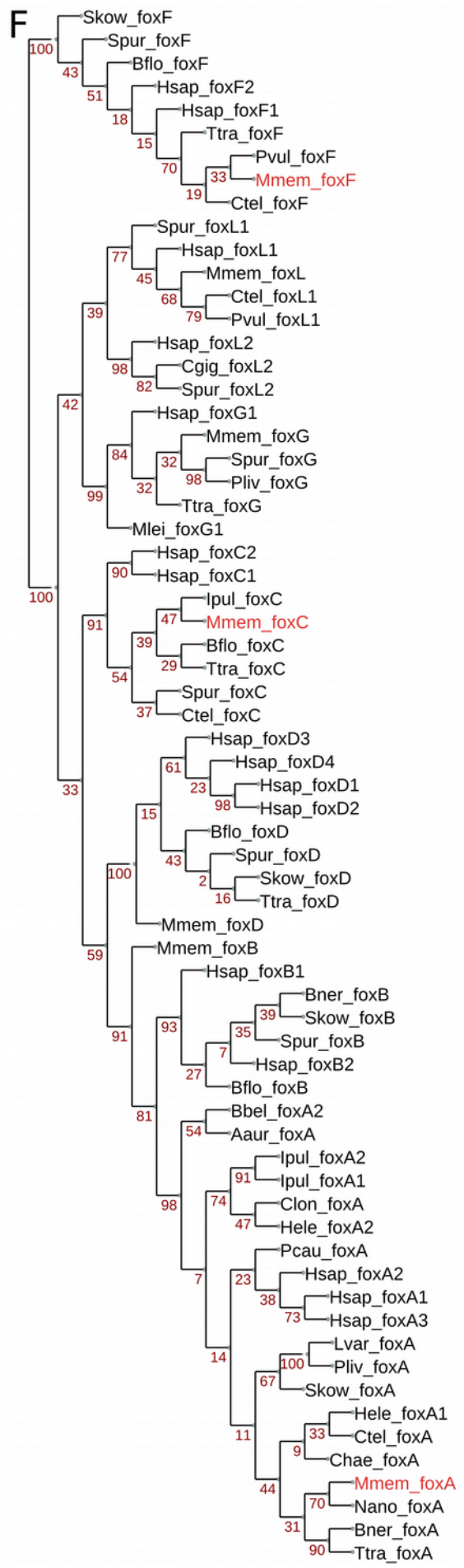

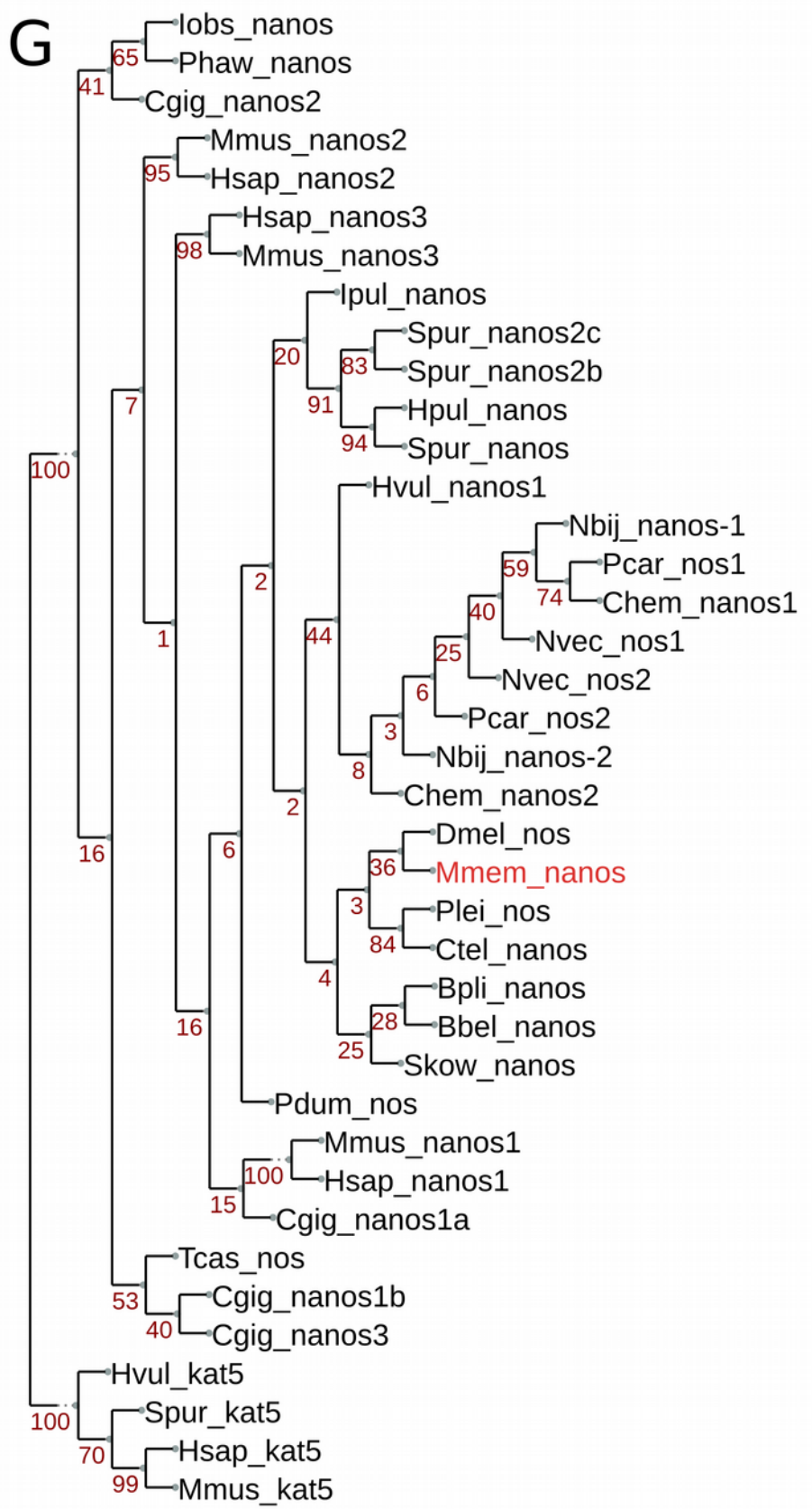

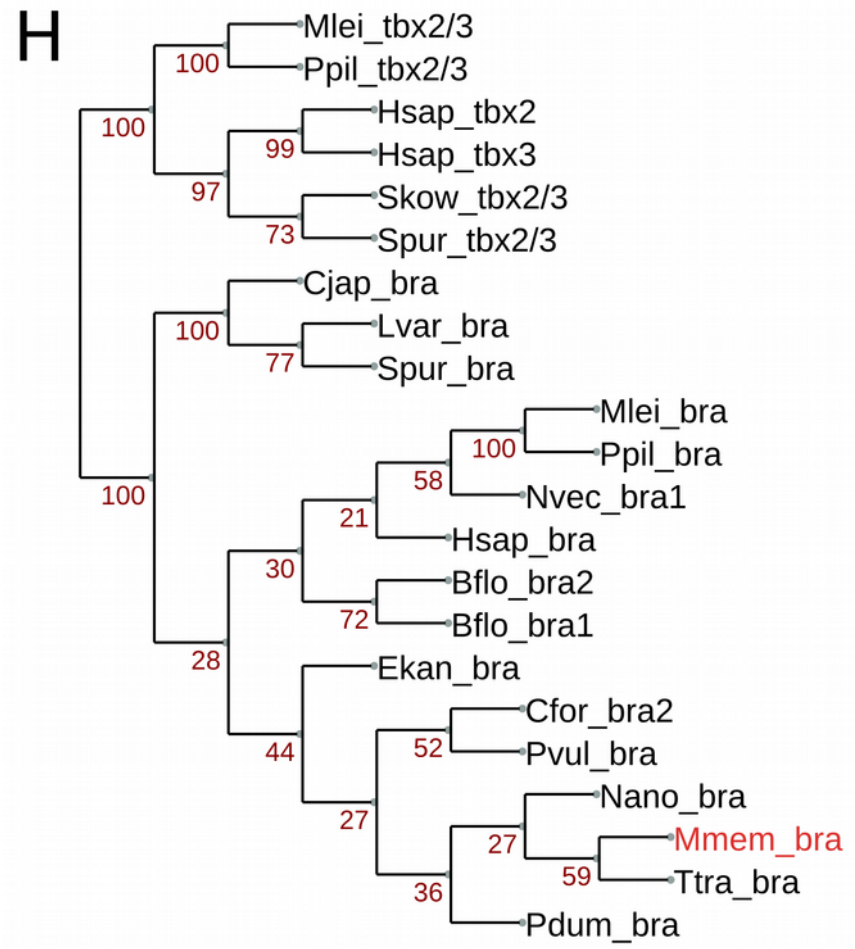

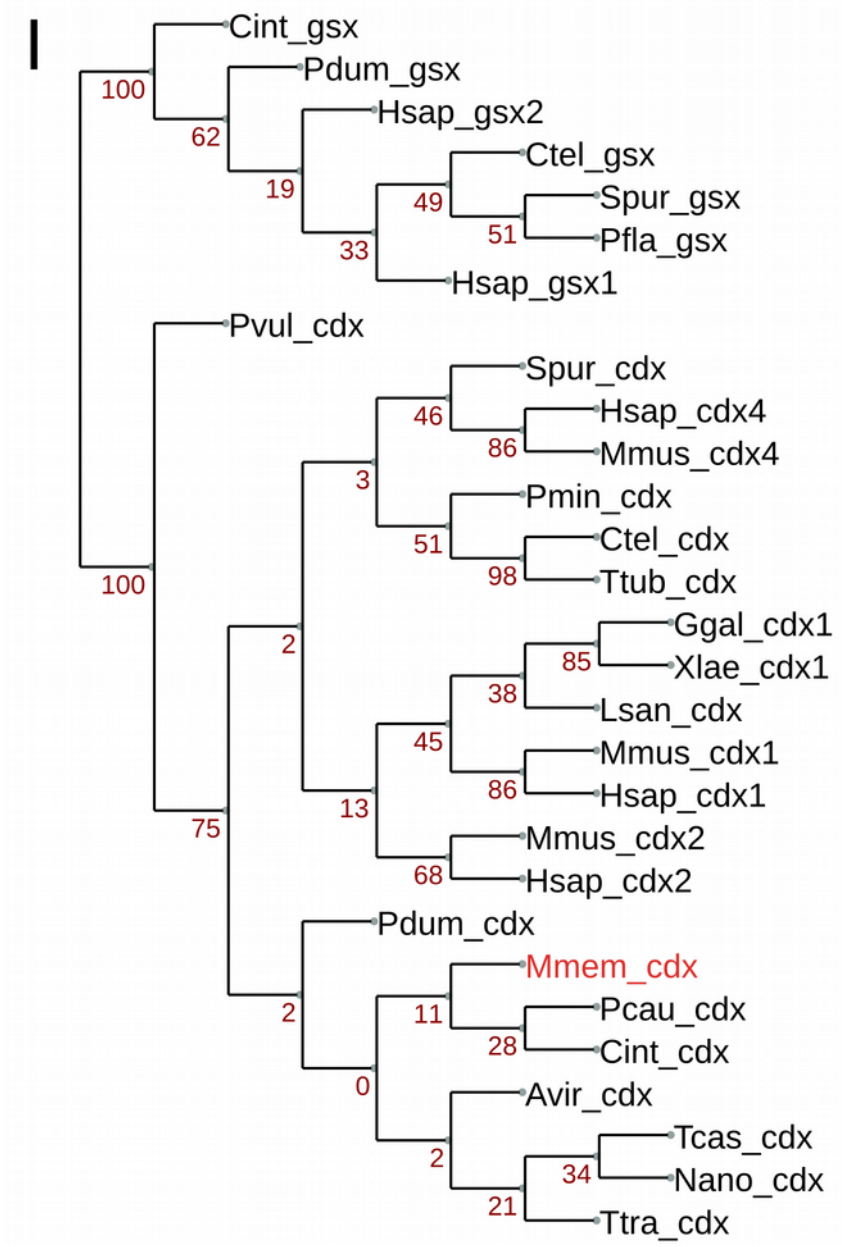

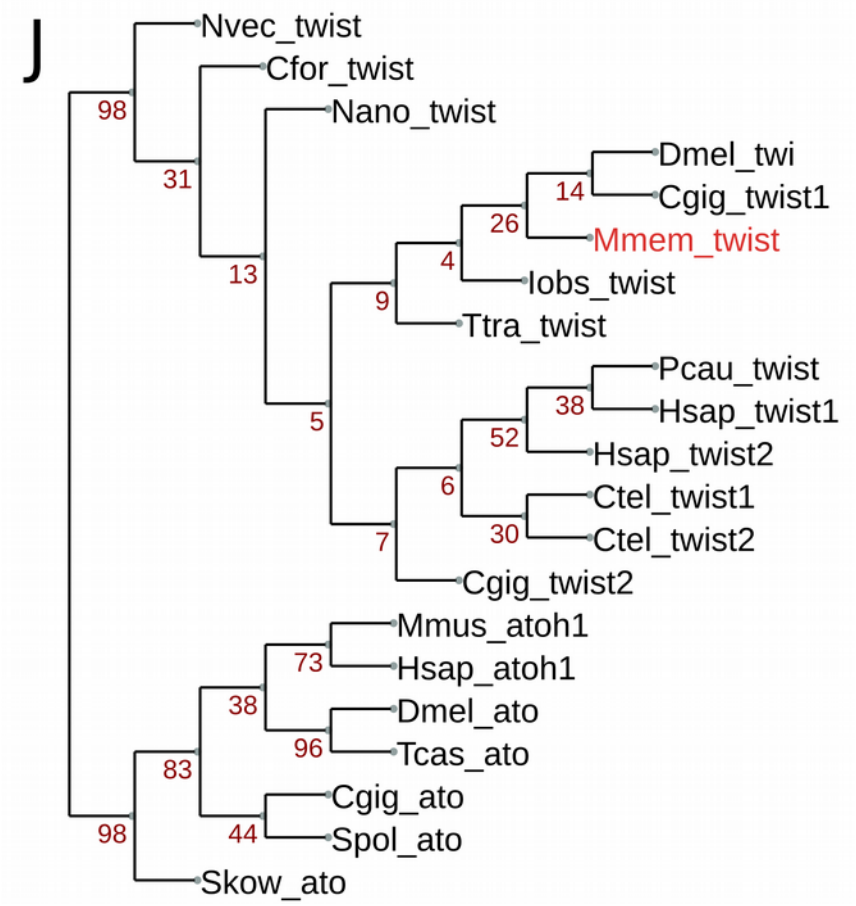

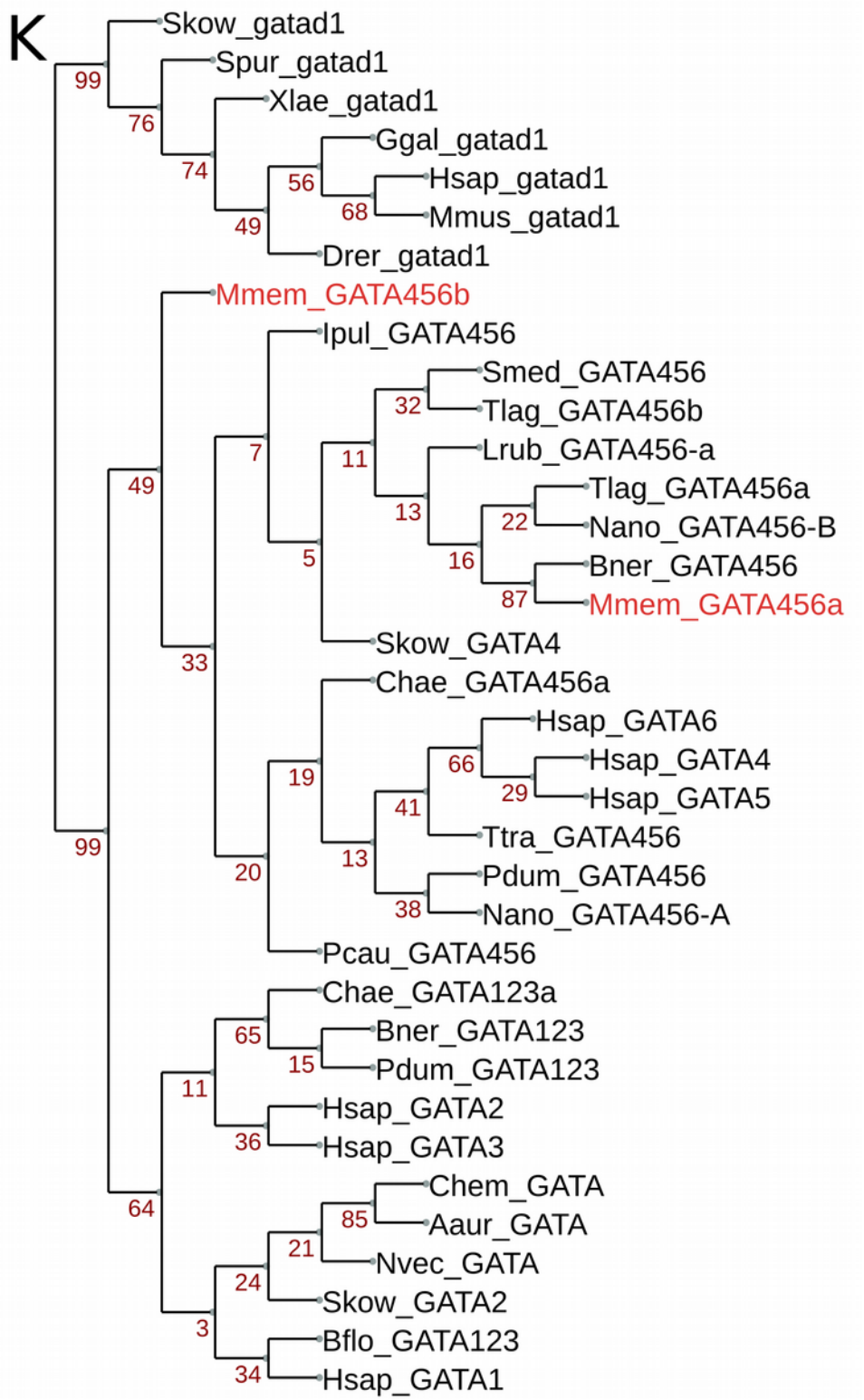

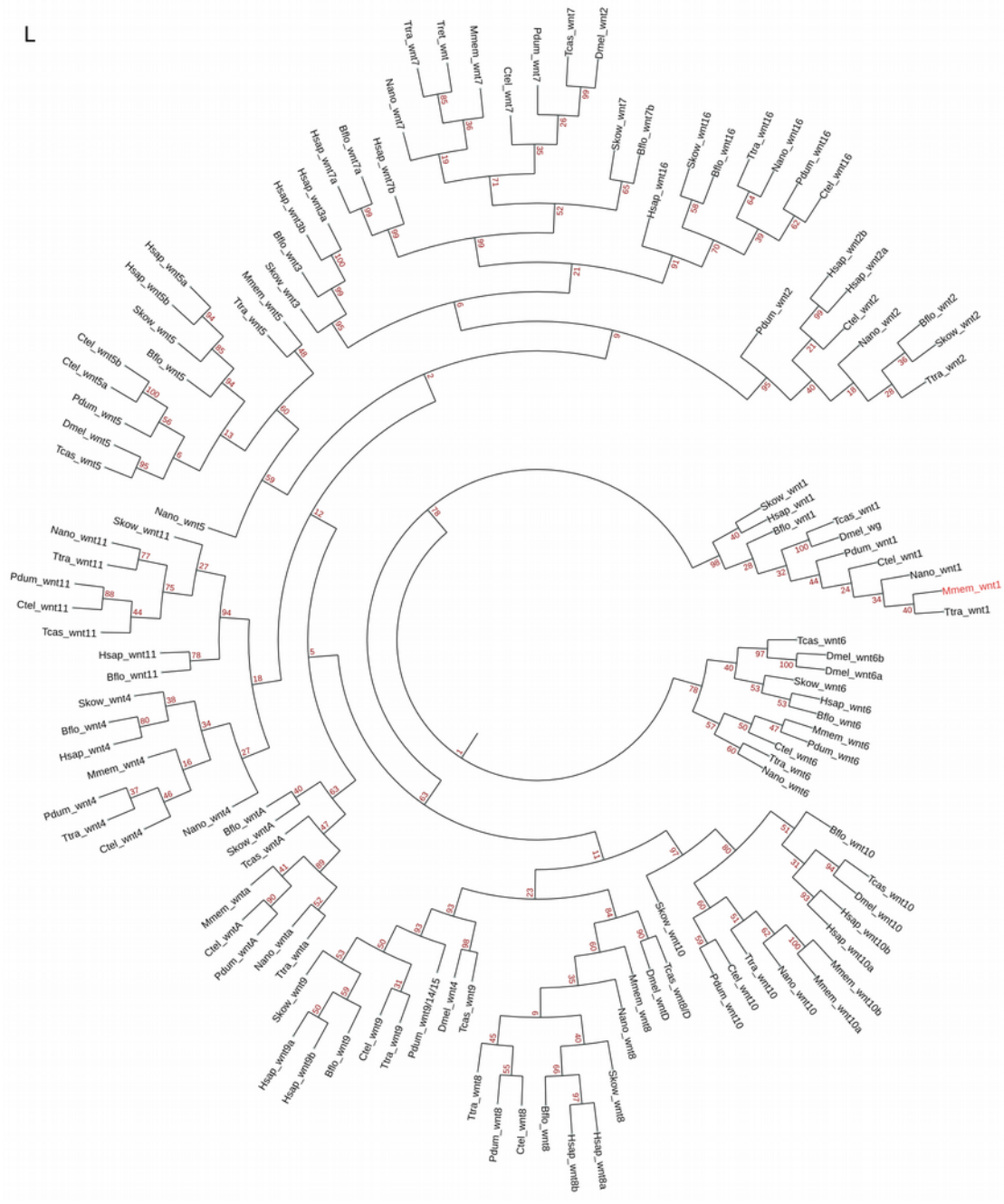

Figure S5. Orthology assignment for the bryozoan genes used in this study. (A) *six3/6*, (B) *dlx* and *evx*, (C) *otx* and *gsc*, (D) *pax6*, (E) *nk2.1*, (F) *foxa*, *foxc* and *foxf*, (G) *nanos*, (H) *bra*, (I) *cdx*, (J) *twist*, (K) *gata456*, (L) *wnt1*. Cladograms show branch support values and bryozoan orthologs in red.

Table 1. MAPK activity in spiralians.

taxon	species	ABCD sizes	MAPK activity	MAPK inhibition
Mollusca (gastropod)	*Ilyanassa obsoleta*	Unequal	Strong signal in the cytoplasm around nucleus of the 3D cell. Activity spread on the overlying 2d1 and 2d2; then 1c12, 1a12, 1b12; 4d cell, but not 4D; derivatives of the second and third quartet forming an arc centered in the dorsal midline; micromeres 2b12 and 3b1 transiently; undetectable 6h after 4d formation; never detected in 3A, 3B, 3C, 2b2 or 3a (Lambert and Nagy, 2001).	Disorganized and incomplete larvae. MAPK activation is required on the micromeres themselves, not only in 3D. Alters the cleavage pattern in the third quartet of micromeres and timing of division of the 4d (Lambert and Nagy, 2001).
Mollusca (gastropod)	*Crepidula fornicata*	Equal-like	1a1-1d1 micromeres, fainter in 1a2-1d2; 3D cell, persisting in 4d; also 3d1-3d2 and 1a12-1d12 (Henry and Perry, 2007).	Resulted in radialized embryos with no differentiated axial properties or cell fates (Henry and Perry, 2007).
Mollusca (gastropod)	*Stagnicola palustris* (=*Lymnaea palustris*)*	Equal	3D only (Lambert and Nagy, 2003).	-
Mollusca (gastropod)	*Lottia scutum* (=*Tectura scutum*)*	Equal	3D only (Lambert and Nagy, 2003).	Prevented normal development of micromeres producing the foot, the shell and affecting the differentiation of eyes (Lambert and Nagy, 2003).

Mollusca (gastropod)	*Haliotis asinina*	Equal	3D only (Koop et al., 2007).	Retarded development and failure to develop larval musculature, shell and foot. But gene expression not completely radialized (Koop et al., 2007).
Mollusca (polyplacophoran)	*Chaetopleura apiculata*	Equal	3D only (Lambert and Nagy, 2003).	-
Annelida (sedentary polychaete)	*Hydroides dianthus* (=*Hydroides hexagonus*)*	Equal	4d only (Lambert and Nagy, 2003).	-
Annelida (sedentary polychaete)	*Capitella teleta*	Unequal	Cells around the blastopore during gastrulation (Amiel et al., 2013).	Resulted in compact shape larva with less muscles and disorganized axon tracts, but without affecting the D quadrant specification, organizing activity or establishment of larval body axes (Amiel et al., 2013).
Annelida (errant polychaete)	*Platynereis dumerilii*	Unequal	Two dorsal cells (nephroblasts) and micromeres around the blastopore (Pfeifer et al., 2014).	Shortened overall morphology with disorganized muscle and neural tracts (Pfeifer et al., 2014).
Bryozoa (gymnolaemate)	*Membranipora membranacea*	Equal	3D only.	Reduced larva.

*Synonyms taken from WoRMS database.

Table 2. Gene expression patterns in spiralians.

taxon	***six3/6***	***dlx***	***otx***	***pax6***	***nk2.1***	***foxa***	***gsc***	***nanos***
Rotifera	-	-	-	anterior bilateral patches (Boell and Bucher, 2008)	-	-	-	oocyte and posterior patch of ovary cells (Smith et al., 2010)
Micrognathozoa	-	-	-	-	-	-	-	-
Gnathostomulida	-	-	-	-	-	-	-	-
Platyhelminthes	brain branches (Pineda and Saló, 2002)		brain (Umesono et al., 1999)	eyes (Callaerts et al., 1999)		pharynx duct (Martín-Durán et al., 2010)	central nervous system (Martín-Durán and Romero, 2011)	germline and eye precursors (Handberg-Thorsager and Saló, 2007; Sato et al., 2006)
Gastrotricha	-	-	-	-	-	-	-	-

Mollusca	anterior blastopore lip, apical ganglia and ocelli (Perry et al., 2015)	all animal pole cells and general ectoderm (Lee and Jacobs, 1999)	prototroch (Nederbragt et al., 2002a); blastopore lip, ventral midline, mouth, mesoderm and velum (Perry et al., 2015)	optic region, brain and arms (Tomarev et al., 1997)	anterior most region of the stomodeum, crescent above the mouth (Perry et al., 2015)	blastopore lips, endoderm and mesoderm (Lartillot et al., 2002b; Perry et al., 2015)	anterior mesoderm during gastrulation, foregut and mantle edge in larval stages (Lartillot et al., 2002b); ecto and endomesoderm and anterior of blastopore lip (Perry et al., 2015)	animal pole cells than two posterior bilaterally symmetrical cells (Kranz et al., 2010); or 4d (Rabinowitz et al., 2008)
Annelida	apical domain encircling apical organ (Marlow et al., 2014; Steinmetz et al., 2010)	apical ectoderm, apical organ, prototroch and ganglia (McDougall et al., 2011)	early apical organ, foregut and prototroch (Arendt et al., 2001; Marlow et al., 2014; Steinmetz et al., 2010), also brain and posterior growth zone (Boyle et al., 2014)	anterior bilateral patches (Arendt et al., 2002; Denes et al., 2007; Quigley et al., 2007)	apical ventral domain above prototroch (Marlow et al., 2014) and bilateral domains flanking blastopore (Boyle et al., 2014)	vegetal plate ring with cleared posterior expression, foregut and hindgut (Arenas-Mena, 2006; Boyle and Seaver, 2008; Boyle and Seaver, 2010; Boyle et al., 2014)	foregut and bilateral neural domains (Arendt et al., 2001; Boyle et al., 2014)	mesodermal posterior growth zone (Rebscher et al., 2007); anterior ectodermal clusters, foregut, posterior segmental zone (Dill and Seaver, 2008)

Nemertea	apical organ, ciliary band and cephalic imaginal discs (Hiebert and Maslakova, 2015a), anterior invagination and apical disc (Hiebert and Maslakova, 2015b)	-	-	-	-	-	-	-
Brachiopoda	apical domain (Santagata et al., 2012)	mantle lobe	apical domain	apical lobe	anteroventral	-	mouth	pedicle mesoderm
Phoronida	-	-	-	-	-	-	-	-
Entoprocta	-	-	-	-	-	-	-	-
Bryozoa	apical organ, anterior endoderm and lateral vegetal plate cell	apical organ	corona, apical disc during gastrulation	bilateral domains above the corona	vegetal anterior domain below corona	anterior vestibule ectoderm (oral ectoderm?)	two anterior vegetal cells and pair of bilateral domains	two posterior cells on the vegetal plate

Table 2 (continued). Gene expression patterns in spiralians.

taxon	*bra*	*cdx*	*evx*	*wnt1*	*twist*	*foxc*	*foxf*	*gata456*
Rotifera	-	-	-	-	-	-	-	-
Micrognatho-zoa	-	-	-	-	-	-	-	-
Gnathosto-mulida	-	-	-	-	-	-	-	-
Platy-helminthes					pharynx mus-cle (Martín-Durán et al., 2010)			
Gastrotricha	-	-	-	-	-	-	-	-
Mollusca	3D and mostly poste-rior edge of the blastopore (Lartillot et al., 2002a; Perry et al., 2015)	posterior ecto-derm, meso-derm close to the blastopore (Le Gouar et al., 2003; Perry et al., 2015) and mouth/esoph-agus (Perry et al., 2015)	-	-	anterior meso-derm but not in its mes-enchymal progeny (Nederbragt et al., 2002b; Perry et al., 2015)	-	-	-
Annelida	A-D macromeres, foregut and hindgut (Arendt et al., 2001; Boyle et al., 2014)	hindgut, pos-terior end (Rosa et al., 2005; Samadi and Steiner, 2010)	posterior and bilateral bands that can be internal-ized (Rosa et al., 2005)	posterior end (Prud'homme et al., 2003; Seaver and Kaneshige, 2006)	mesoderm derivatives during larval development (Dill et al., 2007; Pfeifer et al., 2013)	-	-	endomeso-derm in paired lateral bands (Gillis et al., 2007)

Nemertea	-	posterior most end, then subepidermal (Hiebert and Maslakova, 2015b)	-	-	-	-	-	-
Brachiopoda	anus	anus and posterior mesoderm	posterior end	posterior end of blastopore	ring in archenteron wall and anterior mesoderm (Passamaneck et al., 2015)	apical and pedicle mesoderm (Passamaneck et al., 2015)	anterior mesoderm (Passamaneck et al., 2015)	endoderm and posterior mesoderm (Passamaneck et al., 2015)
Phoronida	-	-	-	-	-	-	-	-
Entoprocta	-	-	-	-	-	-	-	-
Bryozoa	posterior domain not directly surrounding the blastopore; likely hindgut, maybe posterior mesoderm?	domain posterior to the blastopore, larval hindgut	single posterior ectodermal cell, bilateral vegetal blastomeres, larval hindgut	few posterior cells on vegetal side, posterior ectoderm	bilateral inner blastomeres during mid gastrulation, maybe anterior in the larva, maybe just absent	one posterior ectodermal cell, divides in two cells during mid gastrulation, future internal sac region	single cell derivative of anterior blastomere, anterior larval mesoderm	posterior vegetal blastomere, larval gut

References

Ackermann, C., Dorresteijn, A. and Fischer, A. (2005). Clonal domains in postlarval *Platynereis dumerilii* (Annelida: Polychaeta). *J. Morphol.* **266**, 258–280.

Amiel, A. R., Henry, J. Q. and Seaver, E. C. (2013). An organizing activity is required for head patterning and cell fate specification in the polychaete annelid *Capitella teleta*: New insights into cell-cell signaling in Lophotrochozoa. *Dev. Biol.* **379**, 107–122.

Arenas-Mena, C. (2006). Embryonic expression of *HeFoxA1* and *HeFoxA2* in an indirectly developing polychaete. *Dev. Genes Evol.* **216**, 727–736.

Arendt, D., Technau, U. and Wittbrodt, J. (2001). Evolution of the bilaterian larval foregut. *Nature* **409**, 81–85.

Arendt, D., Tessmar, K., Campos-Baptista, M.-I. M. de, Dorresteijn, A. and Wittbrodt, J. (2002). Development of pigment-cup eyes in the polychaete *platynereis dumerilii* and evolutionary conservation of larval eyes in bilateria. *Development* **129**, 1143–1154.

Asadulina, A., Panzera, A., Verasztó, C., Liebig, C. and Jékely, G. (2012). Whole-body gene expression pattern registration in *Platynereis* larvae. *Evodevo* **3**, 27.

Barrois, J. (1877). Recherches sur l'embryologie des bryozoaires. *Trav. Stn. Zool. Wimereux* **1**, 1–305.

Biggelaar, J. A. van den (1977). Development of dorsoventral polarity and mesentoblast determination in *Patella vulgata*. *J. Morphol.* **154**, 157–186.

Boell, L. A. and Bucher, G. (2008). Whole-mount in situ hybridization in the rotifer *Brachionus plicatilis* representing a basal branch of lophotrochozoans. *Dev. Genes Evol.* **218**, 445–451.

Boyer, B. C., Henry, J. Q. and Martindale, M. Q. (1996). Dual origins of mesoderm in a basal spiralian: Cell lineage analyses in the polyclad turbellarian *Hoploplana inquilina*. *Dev. Biol.* **179**, 329–338.

Boyer, B. C., Henry, J. J. and Martindale, M. Q. (1998). The cell lineage of a polyclad turbellarian embryo reveals close similarity to coelomate spiralians. *Dev. Biol.* **204**, 111–123.

Boyle, M. J. and Seaver, E. C. (2008). Developmental expression of *foxA* and *gata* genes during gut formation in the polychaete annelid, *Capitella* sp. I. *Evol. Dev.* **10**, 89–105.

Boyle, M. J. and Seaver, E. C. (2010). Expression of *FoxA* and *GATA* transcription factors correlates with regionalized gut development in two lophotrochozoan marine worms: *Chaetopterus* (Annelida) and *Themiste lageniformis* (Sipuncula). *Evodevo* **1**, 2.

Boyle, M. J., Yamaguchi, E. and Seaver, E. C. (2014). Molecular conservation of metazoan gut formation: Evidence from expression of endomesoderm genes in *Capitella teleta* (Annelida). *Evodevo* **5**, 39.

Callaerts, P., Munoz-Marmol, A. M., Glardon, S., Castillo, E., Sun, H., Li, W.-H., Gehring, W. J. and Salo, E. (1999). Isolation and expression of a *pax-6* gene in the regenerating and intact planarian *Dugesia(G)tigrina*. *Proceedings of the National Academy of Sciences* **96**, 558–563.

Calvet, L. (1900). *Contributions à l'histoire naturelle des bryozoaires ectoproctes marins*. Travaux de l'Institut de Zoologie de l'Université de Montpellier.

Child, C. M. (1897). A preliminary account of the cleavage of *Arenicola cristata*, with remarks on the mosaic theory. *Zoological Bulletin*.

Child, C. M. (1900). The early development of *Arenicola* and *Sternaspis*. *Wilhelm Roux Arch. Entwickl. Mech. Org.* **9**, 587–723.

Clement, A. C. (1952). Experimental studies on germinal localization in *Ilyanassa*. I. The role of the polar lobe in determination of the cleavage pattern and its influence in later development. *J. Exp. Zool.* **121**, 593–625.

Clement, A. C. (1962). Development of *Ilyanassa* following removal of the D macromere at successive cleavage stages. *J. Exp. Zool.* **149**, 193–215.

Conklin, E. G. (1897). The embryology of *Crepidula*, A contribution to the cell lineage and early development of some marine gasteropods. *J. Morphol.* **13**, 1–226.

Corrêa, D. D. (1948). A embriologia de *Bugula flabellata* (J. V. Thompson) (Bryozoa Ectoprocta). *Bol. Fac. Fil. Ciênc. e Letr. Univ. São Paulo - Zoologia* **13**, 7–71.

Damen, P. and Dictus, W. J. (1994). Cell lineage of the prototroch of *Patella vulgata* (Gastropoda, Mollusca). *Dev. Biol.* **162**, 364–383.

Davison, A., McDowell, G. S., Holden, J. M., Johnson, H. F., Koutsovoulos, G. D., Liu, M. M., Hulpiau, P., Van Roy, F., Wade, C. M., Banerjee, R., et al. (2016). Formin Is Associated with Left-Right Asymmetry in the Pond Snail and the Frog. *Curr. Biol.* **26**, 654–660.

Denes, A. S., Jékely, G., Steinmetz, P. R. H., Raible, F., Snyman, H., Prud'homme, B., Ferrier, D. E. K., Balavoine, G. and Arendt, D. (2007). Molecular architecture of annelid nerve cord supports common origin of nervous system centralization in Bilateria. *Cell* **129**, 277–288.

Dill, K. K. and Seaver, E. C. (2008). *Vasa* and *nanos* are coexpressed in somatic and germ line tissue from early embryonic cleavage stages through adulthood in the polychaete *Capitella* sp. I. *Dev. Genes Evol.* **218**, 453–463.

Dill, K. K., Thamm, K. and Seaver, E. C. (2007). Characterization of *twist* and *snail* gene expression during mesoderm and nervous system development in the polychaete annelid *Capitella* sp. I. *Dev. Genes Evol.* **217**, 435–447.

Dunn, C. W., Giribet, G., Edgecombe, G. D. and Hejnol, A. (2014). Animal phylogeny and its evolutionary implications. *Annu. Rev. Ecol. Evol. Syst.* **45**, 371–395.

d'Hondt, J.-L. (1983). Sur l'évolution des quatre macromères du pôle végétatif chez les embryons de Bryozoaires Eurystomes. *Cah. Biol. Mar.* **23**, 177–185.

Eisig, H. (1898). Zur Entwicklungsgeschichte der Capitelliden. *Mittheilungen Aus der Zoologischen Station Zu Neapel* **13**, 1–292.

Extavour, C. G. M. and Akam, M. (2003). Mechanisms of germ cell specification across the metazoans: Epigenesis and preformation. *Development* **130**, 5869–5884.

Freeman, G. and Lundelius, J. W. (1992). Evolutionary implications of the mode of D quadrant specification in coelomates with spiral cleavage. *J. Evol. Biol.* **5**, 205–247.

Gillis, W. J., Bowerman, B. and Schneider, S. Q. (2007). Ectoderm- and endomesoderm-specific GATA transcription factors in the marine annelid *Platynereis dumerilli*. *Evol. Dev.* **9**, 39–50.

Gline, S. E., Nakamoto, A., Cho, S.-J., Chi, C. and Weisblat, D. A. (2011). Lineage analysis of micromere 4d, a super-phylotypic cell for Lophotrochozoa, in the leech *Helobdella* and the sludgeworm *Tubifex*. *Dev. Biol.* **353**, 120–133.

Gonzales, E. E., Zee, M. van der, Dictus, W. J. A. G. and Biggelaar, J. van den (2006). Brefeldin A or monensin inhibits the 3D organizer in gastropod, polyplacophoran, and scaphopod molluscs. *Dev. Genes Evol.* **217**, 105–118.

Goulding, M. Q. (2009). Cell lineage of the *Ilyanassa* embryo: Evolutionary acceleration of regional differentiation during early development. *PLoS One* **4**, e5506.

Grabherr, M. G., Haas, B. J., Yassour, M., Levin, J. Z., Thompson, D. a, Amit, I., Adiconis, X., Fan, L., Raychowdhury, R., Zeng, Q., et al. (2011). Full-length transcriptome assembly from RNA-Seq data without a reference genome. *Nat. Biotechnol.* **29**, 644–652.

Gruhl, A. (2009). Ultrastructure of mesoderm formation and development in *Membranipora membranacea* (Bryozoa: Gymnolaemata). *Zoomorphology* **129**, 45–60.

Guralnick, R. P. and Lindberg, D. R. (2001). Reconnecting cell and animal lineages: What do cell lineages tell us about the evolution and development of Spiralia? *Evolution* **55**, 1501–1519.

Handberg-Thorsager, M. and Saló, E. (2007). The planarian *nanos*-like gene smednos is expressed in germline and eye precursor cells during development and regeneration. *Dev. Genes Evol.* **217**, 403–411.

Häcker, U., Kaufmann, E., Hartmann, C., Jürgens, G., Knöchel, W. and Jäckle, H. (1995). The *Drosophila* fork head domain protein crocodile is required for the establishment of head structures. *EMBO J.* **14**, 5306–5317.

Hejnol, A. (2010). A twist in time–the evolution of spiral cleavage in the light of animal phylogeny. *Integr. Comp. Biol.* **50**, 695–706.

Hejnol, A. and Schnabel, R. (2006). What a couple of dimensions can do for you: Comparative developmental studies using 4D microscopy—examples from tardigrade development. *Integr. Comp. Biol.* **46**, 151–161.

Hejnol, A., Martindale, M. Q. and Henry, J. Q. (2007). High-resolution fate map of the snail *Crepidula fornicata*: The origins of ciliary bands, nervous system, and muscular elements. *Dev. Biol.* **305**, 63–76.

Henry, J. J. and Martindale, M. Q. (1998). Conservation of the spiralian developmental program: Cell lineage of the nemertean, *Cerebratulus lacteus*. *Dev. Biol.* **201**, 253–269.

Henry, J. and Martindale, M. Q. (1999). Conservation and innovation in spiralian development. *Hydrobiologia* 255–265.

Henry, J. J. and Perry, K. J. (2007). MAPK activation and the specification of the D quadrant in the gastropod mollusc, *Crepidula fornicata*. *Dev. Biol.* **313**, 181–195.

Henry, J. J., Klueg, K. M. and Raff, R. A. (1992). Evolutionary dissociation between cleavage, cell lineage and embryonic axes in sea urchin embryos. *Development* **114**, 931–938.

Henry, J. Q., Okusu, A. and Martindale, M. Q. (2004). The cell lineage of the polyplacophoran, *Chaetopleura apiculata*: variation in the spiralian program and implications for molluscan evolution. *Dev. Biol.* **272**, 145–160.

Henry, J. Q., Hejnol, A., Perry, K. J. and Martindale, M. Q. (2007). Homology of ciliary bands in Spiralian Trochophores. *Integr. Comp. Biol.* **47**, 865–871.

Hiebert, L. S. and Maslakova, S. A. (2015a). Hox genes pattern the anterior-posterior axis of the juvenile but not the larva in a maximally indirect developing invertebrate, *Micrura alaskensis* (Nemertea). *BMC Biol.* **13**, 23.

Hiebert, L. S. and Maslakova, S. A. (2015b). Expression of *Hox*, *Cdx*, and *Six3/6* genes in the hoplonemertean *Pantinonemertes californiensis* offers insight into the evolution of maximally indirect development in the phylum Nemertea. *Evodevo* **6**, 26.

Huerta-Cepas, J., Dopazo, J. and Gabaldón, T. (2010). ETE: A python Environment for Tree Exploration. *BMC Bioinformatics* **11**, 24.

Hyman, L. H. (1959). The lophophorate Coelomates—Phylum ectoprocta. In *The invertebrates: Smaller coelomate groups*, pp. 275–501. New York: McGraw-Hill Book Company, Inc.

Jékely, G. and Arendt, D. (2007). Cellular resolution expression profiling using confocal detection of NBT/BCIP precipitate by reflection microscopy. *Biotechniques* **42**, 751–755.

Juliano, C. E., Swartz, S. Z. and Wessel, G. M. (2010). A conserved germline multipotency program. *Development* **137**, 4113–4126.

Katoh, K. and Standley, D. M. (2013). MAFFT multiple sequence alignment software version 7: Improvements in performance and usability. *Mol. Biol. Evol.* **30**, 772–780.

Koop, D., Richards, G. S., Wanninger, A., Gunter, H. M. and Degnan, B. M. (2007). The role of MAPK signaling in patterning and establishing axial symmetry in the gastropod *Haliotis asinina*. *Dev. Biol.* **311**, 200–212.

Kozin, V. V., Filimonova, D. A., Kupriashova, E. E. and Kostyuchenko, R. P. (2016). Mesoderm patterning and morphogenesis in the polychaete *Alitta virens* (Spiralia, Annelida): Expression of mesodermal markers *Twist*, *Mox*, *Evx* and functional role for MAP kinase signaling. *Mech. Dev.* **140**, 1–11.

Kranz, A. M., Tollenaere, A., Norris, B. J., Degnan, B. M. and Degnan, S. M. (2010). Identifying the germline in an equally cleaving mollusc: *Vasa* and *Nanos* expression during embryonic and larval development of the vetigastropod *Haliotis asinina*. *J. Exp. Zool. B Mol. Dev. Evol.* **314**, 267–279.

Kuroda, R. (2015). A twisting story: how a single gene twists a snail? Mechanogenetics. *Q. Rev. Biophys.* **48**, 445–452.

Lacalli, T. C. (1981). Structure and development of the apical organ in trochophores of *Spirobranchus polycerus*, *Phyllodoce maculata* and *Phyllodoce mucosa* (Polychaeta). *Proceedings of the Royal Society of London B: Biological Sciences* **212**, 381–402.

Lambert, J. D. (2008). Mesoderm in spiralians: the organizer and the 4d cell. *J. Exp. Zool. B Mol. Dev. Evol.* **310**, 15–23.

Lambert, J. D. (2010). Developmental patterns in spiralian embryos. *Curr. Biol.* **20**, R72–7.

Lambert, J. D. and Nagy, L. M. (2001). MAPK signaling by the D quadrant embryonic organizer of the mollusc *Ilyanassa obsoleta*. *Development* **128**, 45–56.

Lambert, J. D. and Nagy, L. M. (2003). The MAPK cascade in equally cleaving spiralian embryos. *Dev. Biol.* **263**, 231–241.

Lartillot, N., Lespinet, O., Vervoort, M. and Adoutte, A. (2002a). Expression pattern of *Brachyury* in the mollusc *Patella vulgata* suggests a conserved role in the establishment of the AP axis in Bilateria. *Development* **129**, 1411–1421.

Lartillot, N., Le Gouar, M. and Adoutte, A. (2002b). Expression patterns of *fork head* and *goosecoid* homologues in the mollusc *Patella vulgata* supports the ancestry of the anterior mesendoderm across Bilateria. *Dev. Genes Evol.* **212**, 551–561.

Laumer, C. E., Bekkouche, N., Kerbl, A., Goetz, F., Neves, R. C., Sørensen, M. V., Kristensen, R. M., Hejnol, A., Dunn, C. W., Giribet, G., et al. (2015). Spiralian phylogeny informs the evolution of microscopic lineages. *Curr. Biol.* **25**, 2000–2006.

Le Gouar, M., Lartillot, N., Adoutte, A. and Vervoort, M. (2003). The expression of a *caudal* homologue in a mollusc, *Patella vulgata*. *Gene Expr. Patterns* **3**, 35–37.

Lee, S. E. and Jacobs, D. K. (1999). Expression of *Distal-less* in molluscan eggs, embryos, and larvae. *Evol. Dev.* **1**, 172–179.

Lillie, F. R. (1895). The embryology of the Unionidae. A study in cell-lineage. *J. Morphol.* **10**, 1–100.

Long, J. A. and Stricker, S. A. (1991). Brachiopoda. In *Reproduction of Marine Invertebrates: Echinoderms and Lophophorates* (ed. Giese, A. C.), Pearse, J. S.), and Pearse, V. B.), pp. 47–84. The Boxwood Press.

Lowe, C. J., Wu, M., Salic, A., Evans, L., Lander, E., Stange-Thomann, N., Gruber, C. E., Gerhart, J. and Kirschner, M. (2003). Anteroposterior patterning in hemichordates and the origins of the chordate nervous system. *Cell* **113**, 853–865.

Lyons, D. C. and Henry, J. Q. (2014). Ins and outs of Spiralian gastrulation. *Int. J. Dev. Biol.* **58**, 413–428.

Lyons, D. C., Perry, K. J., Lesoway, M. P. and Henry, J. Q. (2012). Cleavage pattern and fate map of the mesentoblast, 4d, in the gastropod *Crepidula*: a hallmark of spiralian development. *Evodevo* **3**, 21.

Marcus, E. (1938). Bryozoarios Marinhos Brasileiros II. *Bol. Fac. Phil., Sc. Letr. Univ. S. Paulo, Zoologia* **2**, 3–137.

Marcus, E. (1939). Bryozoarios Marinhos Brasileiros III. *Bol. Fac. Phil., Sc. Letr. Univ. S. Paulo, Zoologia* **3**, 113–299.

Marlow, H., Tosches, M. A., Tomer, R., Steinmetz, P. R., Lauri, A., Larsson, T. and Arendt, D. (2014). Larval body patterning and apical organs are conserved in animal evolution. *BMC Biol.* **12**, 7.

Martindale, M. Q. (1986). The "organizing" role of the D quadrant in an equal-cleaving spiralian, lymnaea stagnalis as studied by UV laser deletion of macromeres at intervals between third and fourth quartet formation. *International Journal of Invertebrate Reproduction and Development* **9**, 229–242.

Martindale, M. Q. and Henry, J. Q. (1995). Modifications of cell fate specification in equal-cleaving nemertean embryos: Alternate patterns of spiralian development. *Development* **121**, 3175–3185.

Martindale, M. Q., Doe, C. Q. and Morrill, J. B. (1985). The role of animal-vegetal interaction with respect to the determination of dorsoventral polarity in the equal-cleaving spiralian, *Lymnaea palustris*. *Wilhelm Roux Arch. Entwickl. Mech. Org.* **194**, 281–295.

Martín-Durán, J. M. and Egger, B. (2012). Developmental diversity in free-living flatworms. *Evodevo* **3**, 7.

Martín-Durán, J. M. and Romero, R. (2011). Evolutionary implications of morphogenesis and molecular patterning of the blind gut in the planarian *Schmidtea polychroa*. *Dev. Biol.* **352**, 164–176.

Martín-Durán, J. M., Amaya, E. and Romero, R. (2010). Germ layer specification and axial patterning in the embryonic development of the freshwater planarian *Schmidtea polychroa*. *Dev. Biol.* **340**, 145–158.

Martín-Durán, J. M., Janssen, R., Wennberg, S., Budd, G. E. and Hejnol, A. (2012). Deuterostomic development in the protostome *Priapulus caudatus*. *Curr. Biol.* **22**, 2161–2166.

Martín-Durán, J. M., Vellutini, B. C. and Hejnol, A. (2015). Evolution and development of the adelphophagic, intracapsular Schmidt's larva of the nemertean *Lineus ruber*. *Evodevo* **6**, 28.

Maslakova, S. A., Martindale, M. Q. and Norenburg, J. L. (2004a). Vestigial prototroch in a basal nemertean, *Carinoma tremaphoros* (Nemertea; Palaeonemertea). *Evol. Dev.* **6**, 219–226.

Maslakova, S. A., Martindale, M. Q. and Norenburg, J. L. (2004b). Fundamental properties of the spiralian developmental program are displayed by the basal nemertean *Carinoma tremaphoros* (palaeonemertea, nemertea). *Dev. Biol.* **267**, 342–360.

Mazet, F., Amemiya, C. T. and Shimeld, S. M. (2006). An ancient Fox gene cluster in bilaterian animals. *Curr. Biol.* **16**, R314–6.

McDougall, C., Korchagina, N., Tobin, J. L. and Ferrier, D. E. (2011). Annelid *Distal-less/Dlx* duplications reveal varied post-duplication fates. *BMC Evol. Biol.* **11**, 241.

Mead, A. D. (1897). The early development of marine annelids. *J. Morphol.* **13**, 227–326.

Merkel, J., Wollesen, T., Lieb, B. and Wanninger, A. (2012). Spiral cleavage and early embryology of a loxosomatid entoproct and the usefulness of spiralian apical cross patterns for phylogenetic inferences. *BMC Dev. Biol.* **12**, 11.

Meyer, N. P., Boyle, M. J., Martindale, M. Q. and Seaver, E. C. (2010). A comprehensive fate map by intracellular injection of identified blastomeres in the marine polychaete *Capitella teleta*. *Evodevo* **1**, 8.

Nederbragt, A. J., Welscher, P. te, Driesche, S. van den, Loon, A. E. van and Dictus, W. J. A. G. (2002a). Novel and conserved roles for *orthodenticle/ otx* and *orthopedia/ otp* orthologs in the gastropod mollusc *Patella vulgata*. *Dev. Genes Evol.* **212**, 330–337.

Nederbragt, A. J., Lespinet, O., Wageningen, S. van, Loon, A. E. van, Adoutte, A. and Dictus, W. J. A. G. (2002b). A lophotrochozoan *twist* gene is expressed in the ectomesoderm of the gastropod mollusk *Patella vulgata*. *Evol. Dev.* **4**, 334–343.

Nielsen, C. (2004). Trochophora larvae: Cell-lineages, ciliary bands, and body regions. 1. Annelida and Mollusca. *J. Exp. Zool. B Mol. Dev. Evol.* **302**, 35–68.

Nielsen, C. (2005). Trochophora larvae: Cell-lineages, ciliary bands and body regions. 2. Other groups and general discussion. *J. Exp. Zool. B Mol. Dev. Evol.* **304**, 401–447.

Nielsen, C. and Worsaae, K. (2010). Structure and occurrence of cyphonautes larvae (Bryozoa, Ectoprocta). *J. Morphol.* **271**, 1094–1109.

Okonechnikov, K., Golosova, O., Fursov, M. and UGENE team (2012). Unipro UGENE: A unified bioinformatics toolkit. *Bioinformatics* **28**, 1166–1167.

Oliveri, P., Walton, K. D., Davidson, E. H. and McClay, D. R. (2006). Repression of mesodermal fate by *foxa*, a key endoderm regulator of the sea urchin embryo. *Development* **133**, 4173–4181.

Pace, R. M. (1906). On the early stages in the development of *Flustrella hispida* (Fabricius), and on the existence of a “yolk nucleus” in the egg of this form. *Q. J. Microsc. Sci.*

Panganiban, G. and Rubenstein, J. L. R. (2002). Developmental functions of the *Distal-less/Dlx* homeobox genes. *Development* **129**, 4371–4386.

Passamaneck, Y. J., Hejnol, A. and Martindale, M. Q. (2015). Mesodermal gene expression during the embryonic and larval development of the articulate brachiopod *Terebratalia transversa*. *Evodevo* **6**, 10.

Patient, R. K. and McGhee, J. D. (2002). The GATA family (vertebrates and invertebrates). *Curr. Opin. Genet. Dev.* **12**, 416–422.

Pennerstorfer, M. and Scholtz, G. (2012). Early cleavage in *Phoronis muelleri* (Phoronida) displays spiral features. *Evol. Dev.* **14**, 484–500.

Perry, K. J., Lyons, D. C., Truchado-Garcia, M., Fischer, A. H. L., Helfrich, L. W., Johansson, K. B., Diamond, J. C., Grande, C. and Henry, J. Q. (2015). Deployment of regulatory genes during gastrulation and germ layer specification in a model spiralian mollusc *Crepidula*. *Dev. Dyn.*

Pérez Sánchez, C., Casas-Tintó, S., Sánchez, L., Rey-Campos, J. and Granadino, B. (2002). *DmFoxF*, a novel *Drosophila* fork head factor expressed in visceral mesoderm. *Mech. Dev.* **111**, 163–166.

Pfeifer, K., Schaub, C., Wolfstetter, G. and Dorresteijn, A. (2013). Identification and characterization of a twist ortholog in the polychaete annelid *Platynereis dumerilii* reveals mesodermal expression of *Pdu-twist*. *Dev. Genes Evol.* **223**, 319–328.

Pfeifer, K., Schaub, C., Domsch, K., Dorresteijn, A. and Wolfstetter, G. (2014). Maternal inheritance of *twist* and analysis of MAPK activation in embryos of the polychaete annelid *Platynereis dumerilii*. *PLoS One* **9**, e96702.

Pineda, D. and Saló, E. (2002). Planarian *gtsix3*, a member of the six/so gene family, is expressed in brain branches but not in eye cells. *Mech. Dev.* **119 Suppl 1**, S167–71.

Prouho, H. (1892). Contribution a l´histoire des Bryozoaires. *Archives de zoologie experimentale et generale* **2. sér.**, 557–656.

Prud'homme, B., Rosa, R. de, Arendt, D., Julien, J.-F., Pajaziti, R., Dorresteijn, A. W. C., Adoutte, A., Wittbrodt, J. and Balavoine, G. (2003). Arthropod-like expression patterns of *engrailed* and *wingless* in the annelid *Platynereis dumerilii* suggest a role in segment formation. *Curr. Biol.* **13**, 1876–1881.

Quigley, I. K., Xie, X. and Shankland, M. (2007). *Hau-Pax6A* expression in the central nervous system of the leech embryo. *Dev. Genes Evol.* **217**, 459–468.

Rabinowitz, J. S., Chan, X. Y., Kingsley, E. P., Duan, Y. and Lambert, J. D. (2008). Nanos is required in somatic blast cell lineages in the posterior of a mollusk embryo. *Curr. Biol.* **18**, 331–336.

Rebscher, N. (2014). Establishing the germline in spiralian embyos. *Int. J. Dev. Biol.* **58**, 403–411.

Rebscher, N., Zelada-González, F., Banisch, T. U., Raible, F. and Arendt, D. (2007). Vasa unveils a common origin of germ cells and of somatic stem cells from the posterior growth zone in the polychaete *Platynereis dumerilii*. *Dev. Biol.* **306**, 599–611.

Reed, C. G. (1987). Phylum Bryozoa. In *Reproduction and development of marine invertebrates of the northern pacific coast: Data and methods for the study of eggs, embryos, and larvae* (ed. Strathmann, M. F.), pp. 494–510. University of Washington Press.

Reed, C. G. (1991). Bryozoa. In *Reproduction of marine invertebrates* (ed. Giese, A. C.), Pearse, J. S.), and Pearse, V. B.), pp. 85–245. The Boxwood Press.

Render, J. (1997). Cell fate maps in the *Ilyanassa obsoleta* embryo beyond the third division. *Dev. Biol.* **189**, 301–310.

Riedl, R. J. (1969). Gnathostomulida from america. *Science* **163**, 445–452.

Rosa, R. de, Prud'homme, B. and Balavoine, G. (2005). *Caudal* and *even-skipped* in the annelid *Platynereis dumerilii* and the ancestry of posterior growth. *Evol. Dev.* **7**, 574–587.

Rouse, G. W. (1999). Trochophore concepts: Ciliary bands and the evolution of larvae in spiralian metazoa. *Biol. J. Linn. Soc. Lond.*

Samadi, L. and Steiner, G. (2010). Conservation of *ParaHox* genes' function in patterning of the digestive tract of the marine gastropod *Gibbula varia*. *BMC Dev. Biol.* **10**, 74.

Santagata, S., Resh, C., Hejnol, A., Martindale, M. Q. and Passamaneck, Y. J. (2012). Development of the larval anterior neurogenic domains of *Terebratalia transversa* (Brachiopoda) provides insights into the diversification of larval apical organs and the spiralian nervous system. *Evodevo* **3**, 3.

Sato, K., Shibata, N., Orii, H., Amikura, R., Sakurai, T., Agata, K., Kobayashi, S. and Watanabe, K. (2006). Identification and origin of the germline stem cells as revealed by the expression of nanos-related gene in planarians. *Dev. Growth Differ.* **48**, 615–628.

Schindelin, J., Arganda-Carreras, I., Frise, E., Kaynig, V., Longair, M., Pietzsch, T., Preibisch, S., Rueden, C., Saalfeld, S., Schmid, B., et al. (2012). Fiji: An open-source platform for biological-image analysis. *Nat. Methods* **9**, 676–682.

Scholtz, G. (2005). Homology and ontogeny: Pattern and process in comparative developmental biology. *Theory Biosci.* **124**, 121–143.

Schulze, J. and Schierenberg, E. (2011). Evolution of embryonic development in nematodes. *Evodevo* **2**, 18.

Seaver, E. C. and Kaneshige, L. M. (2006). Expression of 'segmentation' genes during larval and juvenile development in the polychaetes *Capitella* sp. I and *H. elegans*. *Dev. Biol.* **289**, 179–194.

Shimamura, K., Hartigan, D. J., Martinez, S., Puelles, L. and Rubenstein, J. L. (1995). Longitudinal organization of the anterior neural plate and neural tube. *Development* **121**, 3923–3933.

Shimeld, S. M., Boyle, M. J., Brunet, T., Luke, G. N. and Seaver, E. C. (2010). Clustered Fox genes in lophotrochozoans and the evolution of the bilaterian Fox gene cluster. *Dev. Biol.* **340**, 234–248.

Sinigaglia, C., Busengdal, H., Leclère, L., Technau, U. and Rentzsch, F. (2013). The bilaterian head patterning gene *six3/6* controls aboral domain development in a cnidarian. *PLoS Biol.* **11**, e1001488.

Smith, J. M., Cridge, A. G. and Dearden, P. K. (2010). Germ cell specification and ovary structure in the rotifer *Brachionus plicatilis*. *Evodevo* **1**, 5.

Stamatakis, A. (2014). RAxML version 8: A tool for phylogenetic analysis and post-analysis of large phylogenies. *Bioinformatics* **30**, 1312–1313.

Staudt, T., Lang, M. C., Medda, R., Engelhardt, J. and Hell, S. W. (2007). 2,2′-Thiodiethanol: A new water soluble mounting medium for high resolution optical microscopy. *Microsc. Res. Tech.* **70**, 1–9.

Steinmetz, P. R. H., Urbach, R., Posnien, N., Eriksson, J., Kostyuchenko, R. P., Brena, C., Guy, K., Akam, M., Bucher, G. and Arendt, D. (2010). *Six3* demarcates the anterior-most developing brain region in bilaterian animals. *Evodevo* **1**, 14.

Stricker, S. A. (1988). Metamorphosis of the marine bryozoan *Membranipora membranacea*: An ultrastructural study of rapid morphogenetic movements. *J. Morphol.* **196**, 53–72.

Stricker, S. A., Reed, C. G. and Zimmer, R. L. (1988). The cyphonautes larva of the marine bryozoan *Membranipora membranacea*. i. General morphology, body wall, and gut. *Can. J. Zool.* **66**, 368–383.

Struck, T. H., Wey-Fabrizius, A. R., Golombek, A., Hering, L., Weigert, A., Bleidorn, C., Klebow, S., Iakovenko, N., Hausdorf, B., Petersen, M., et al. (2014). Platyzoan paraphyly based on phylogenomic data supports a noncoelomate ancestry of Spiralia. *Mol. Biol. Evol.* **31**, 1833–1849.

Surface, F. M. (1907). The Early Development of a Polyclad, *Planocera Inquilina* Wh. *Proceedings of the Academy of Natural Sciences of Philadelphia* **59**, 514–559.

Takacs, C. M., Amore, G., Oliveri, P., Poustka, A. J., Wang, D., Burke, R. D. and Peterson, K. J. (2004). Expression of an NK2 homeodomain gene in the apical ectoderm defines a new territory in the early sea urchin embryo. *Dev. Biol.* **269**, 152–164.

Talavera, G. and Castresana, J. (2007). Improvement of phylogenies after removing divergent and ambiguously aligned blocks from protein sequence alignments. *Syst. Biol.* **56**, 564–577.

Technau, U. (2001). Brachyury, the blastopore and the evolution of the mesoderm. *Bioessays* **23**, 788–794.

Technau, U. and Scholz, C. B. (2003). Origin and evolution of endoderm and mesoderm. *Int. J. Dev. Biol.* **47**, 531–539.

Temkin, M. H. (1994). Gamete spawning and fertilization in the gymnolaemate bryozoan *Membranipora membranacea*. *Biol. Bull.* **187**, 143–155.

Tomarev, S. I., Callaerts, P., Kos, L., Zinovieva, R., Halder, G., Gehring, W. and Piatigorsky, J. (1997). Squid pax-6 and eye development. *Proc. Natl. Acad. Sci. U. S. A.* **94**, 2421–2426.

Treadwell, A. L. (1901). The cytogeny of *Podarke obscura* Verrill. *J. Morphol.* **17**, 399–486.

Umesono, Y., Watanabe, K. and Agata, K. (1999). Distinct structural domains in the planarian brain defined by the expression of evolutionarily conserved homeobox genes. *Dev. Genes Evol.* **209**, 31–39.

Untergasser, A., Cutcutache, I., Koressaar, T., Ye, J., Faircloth, B. C., Remm, M. and Rozen, S. G. (2012). Primer3–new capabilities and interfaces. *Nucleic Acids Res.* **40**, e115–e115.

Valentine, J. W. (1997). Cleavage patterns and the topology of the metazoan tree of life. *Proc. Natl. Acad. Sci. U. S. A.* **94**, 8001–8005.

Venkatesh, T. V., Holland, N. D., Holland, L. Z., Su, M.-T. and Bodmer, R. (1999). Sequence and developmental expression of amphioxus *AmphiNk2–1*: Insights into the evolutionary origin of the vertebrate thyroid gland and forebrain. *Dev. Genes Evol.* **209**, 254–259.

Wadeson, P. H. and Crawford, K. (2003). Formation of the blastoderm and yolk syncytial layer in early squid development. *Biol. Bull.* **205**, 179–180.

Waeschenbach, A., Taylor, P. D. and Littlewood, D. T. J. (2012). A molecular phylogeny of bryozoans. *Mol. Phylogenet. Evol.* **62**, 718–735.

Wanninger, A. ed. (2015). *Evolutionary Developmental Biology of Invertebrates 2: Lophotrochozoa (Spiralia)*. Springer Vienna.

Willems, M., Egger, B., Wolff, C., Mouton, S., Houthoofd, W., Fonderie, P., Couvreur, M., Artois, T. and Borgonie, G. (2009). Embryonic origins of hull cells in the flatworm *Macrostomum lignano* through cell lineage analysis: Developmental and phylogenetic implications. *Dev. Genes Evol.* **219**, 409–417.

Wilson, E. B. (1892). The cell-lineage of *Nereis*. A contribution to the cytogeny of the annelid body. *J. Morphol.* **6**, 361–466.

Wilson, E. B. (1898). Considerations on Cell-lineage and Ancestral Reminiscence, based on a Re-examination of Some Points in the Early Development of Annelids and Polyclades. *Science* **7**, 225–226.

Wilson, E. B. (1903). Experiments on cleavage and localization in the nemertine-egg. *Wilhelm Roux Arch. Entwickl. Mech. Org.* **16**, 411–460.

Wray, G. A. (1994). The evolution of cell lineage in echinoderms. *Am. Zool.* **34**, 353–363.

Zaffran, S., Küchler, A., Lee, H. H. and Frasch, M. (2001). *Biniou* (*FoxF*), a central component in a regulatory network controlling visceral mesoderm development and midgut morphogenesis in *Drosophila*. *Genes Dev.* **15**, 2900–2915.

Zeleny, C. (1904). Experiments on the localization of developmental factors in the nemertine egg. *J. Exp. Zool.* **1**, 293–329.

Zimmer, R. L. (1997). Phoronids, brachiopods, and bryozoans, the lophophorates. In *Embryology: Constructing the organism* (ed. Gilbert, S. F.) and Raunio, A. M.), pp. 279–305. Sinauer Associates, Inc.